N-glycans are direct determinants of CFTR folding and stability in secretory and endocytic membrane traffic

Rina Glozman,[1] Tsukasa Okiyoneda,[4] Cory M. Mulvihill,[4] James M. Rini,[2,3] Herve Barriere,[4] and Gergely L. Lukacs[4]

[1]Hospital for Sick Children Research Institute, [2]Department of Molecular Genetics, and [3]Department of Biochemistry, University of Toronto, Toronto, Ontario, Canada M5G 1X8
[4]Department of Physiology, McGill University, Montreal, Quebec, Canada H3G 1Y6

N-glycosylation, a common cotranslational modification, is thought to be critical for plasma membrane expression of glycoproteins by enhancing protein folding, trafficking, and stability through targeting them to the ER folding cycles via lectin-like chaperones. In this study, we show that N-glycans, specifically core glycans, enhance the productive folding and conformational stability of a polytopic membrane protein, the cystic fibrosis transmembrane conductance regulator (CFTR), independently of lectin-like chaperones. Defective N-glycosylation reduces cell surface expression by impairing both early secretory and endocytic traffic of CFTR. Conformational destabilization of the glycan-deficient CFTR induces ubiquitination, leading to rapid elimination from the cell surface. Ubiquitinated CFTR is directed to lysosomal degradation instead of endocytic recycling in early endosomes mediated by ubiquitin-binding endosomal sorting complex required for transport (ESCRT) adaptors Hrs (hepatocyte growth factor–regulated tyrosine kinase substrate) and TSG101. These results suggest that cotranslational N-glycosylation can exert a chaperone-independent profolding change in the energetic of CFTR in vivo as well as outline a paradigm for the peripheral trafficking defect of membrane proteins with impaired glycosylation.

Introduction

Tightly controlled cellular surveillance mechanisms evolved to ensure that only folded polypeptides enter the distal secretory pathway (Ellgaard and Helenius, 2003; Molinari, 2007; Wiseman et al., 2007). Depending on the polypeptide topology, ER luminal, and transmembrane and/or cytosolic chaperones, cochaperones and folding enzymes assist the co- and posttranslational folding of newly synthesized molecules in the ER (Ellgaard and Helenius, 2003). The folding kinetics and thermodynamics in concert with quality control factors determine whether a polypeptide attains its native conformation or as a terminally unfolded molecule is destined for degradation (Molinari, 2007; Wiseman et al., 2007; Nakatsukasa and Brodsky, 2008).

N-glycosylation is one of the most prevalent posttranslational modifications that occurs during protein synthesis in the ER and has a pivotal role in the folding, targeting, and function of numerous proteins and the degradation of nonnative polypeptides. N-glycosylation is initiated by the cotranslational addition of glucose$_3$-mannose$_9$-*N*-acetylglucosamine$_2$ core oligosaccharides to the Asn residue of the lumenally exposed consensus glycosylation site (NXS/T) by the oligosaccharyltransferase (Helenius and Aebi, 2001; Molinari, 2007). Subsequent trimming of glucose and mannose residues determines whether the polypeptide undergoes additional folding cycles or is targeted for the ER-associated degradation (ERAD) by retrotranslocation and ubiquitin (Ub)-proteasome–dependent proteolysis in the cytosol. Monoglucosylated oligosaccharides are generated by α-glucosidase I and II and recognized by lectin-like ER chaperones (calnexin [CNX] and calreticulin [CRT]). Although additional glycosidase cleavage prevents the rebinding

R. Glozman and T. Okiyoneda contributed equally to this paper.

Correspondence to Gergely L. Lukacs: gergely.lukacs@mcgill.ca

Abbreviations used in this paper: Ab, antibody; BFA, brefeldin A; CAS, castanospermine; CF, cystic fibrosis; CFTR, CF transmembrane conductance regulator; CHX, cycloheximide; CNX, calnexin; CRT, calreticulin; ELAD, endolysosomal degradation; endo, endoglycosidase; ERAD, ER-associated degradation; ESCRT, endosomal sorting complex required for transport; FRIA, fluorescence ratiometric image analysis; LSB, Laemmli sample buffer; MVB, multivesicular body; pH_v, vesicular pH; PNGase, peptide N-glycosidase; TUN, tunicamycin; Ub, ubiquitin; WGA, wheat germ agglutinine; wt, wild type.

The Rockefeller University Press $30.00
J. Cell Biol. Vol. 184 No. 6 847–862
www.jcb.org/cgi/doi/10.1083/jcb.200808124

of native polypeptide to CNX/CRT, incompletely folded conformers are reglucosylated by the folding sensor UDP-glucose/glycoprotein glucosyltransferase to allow additional folding attempts (Helenius and Aebi, 2001; Molinari, 2007). Terminally misfolded glycoproteins are subjected to mannose cleavages and recognition by lectin-like proteins (e.g., EDEMs [ER degradation–enhancing α-mannosidase–like proteins], OS-9, and SEL-1) as adaptor molecules for retrotranslocation (Helenius and Aebi, 2001; Molinari, 2007; Christianson et al., 2008).

N-glycosylation defect can severely impair the cell surface expression of membrane proteins (e.g., rhodopsin, sulphonylurea receptor, and FGF receptor 2), leading to severe diseases such as retinitis pigmentosa, persistent hyperinsulinemic hypoglycemia, and craniosynostosis syndrome, respectively (Conti et al., 2002; Zhu et al., 2004; Mitra et al., 2006). Lack of glycosylation can retard productive folding by preventing client protein engagement with the CNX/CRT cycles and attenuate the metabolic stability at multiple compartments, including the cell surface (Melikian et al., 1996; Gong et al., 2002; Chen et al., 2006). The molecular basis of defective cell surface stability of glycosylation-defective plasma membrane proteins is not known.

Cystic fibrosis (CF) transmembrane conductance regulator (CFTR) is a polytopic integral membrane protein containing two membrane-spanning domains, two nucleotide-binding domains, and a single R domain. Loss of CFTR chloride channel activity at the cell surface causes CF, one of the most common genetic diseases in the Caucasian population (Zielenski and Tsui, 1995). The newly synthesized CFTR undergoes core glycosylation in the fourth extracellular loop and complex-type glycan modification upon traversing the Golgi complex (Cheng et al., 1990; Lukacs et al., 1994; Ward and Kopito, 1994). Only a fraction of the nascent CFTR chains undergoes productive folding, culminating in the formation of protease-resistant transport-competent channels (Lukacs et al., 1994; Ward and Kopito, 1994) that enter COPII transport vesicles (Wang et al., 2004). The conformational maturation of CFTR is assisted by both CNX and cytosolic chaperones (e.g., Hsc70/Hsp70, HdJ1/2, Hsp40, and the Hsp90 complex; Yang et al., 1993; Pind et al., 1994; Loo et al., 1998; Meacham et al., 1999; Okiyoneda et al., 2004; Rosser et al., 2008). The folding of CFTR is attenuated by a large number of point mutations, including the deletion of F508 (ΔF508), the most common CF mutation (Cheng et al., 1990). Although defective N-glycosylation impairs the folding and stability of CFTR (Farinha and Amaral, 2005; Chang et al., 2008), the complex-glycosylated CFTR expression level was modestly reduced in CNX-depleted cells (Farinha and Amaral, 2005; Okiyoneda et al., 2008; Rosser et al., 2008), suggesting that N-glycans may have an intrinsic role in the channel biogenesis.

Using a combination of approaches, we show in this study that besides recruiting CNX and promoting CFTR nascent chain folding, core glycans have a direct effect on channel conformational maturation in the ER. Importantly, although CNX enhances the folding yield without stabilizing the native state, N-glycans structurally stabilize the CFTR as indicated by the decreased protease susceptibility, thermoaggregation, and ubiquitination of the native channel. The structural destabilization provokes the glycan-deficient CFTR ubiquitination. Ubiquitinated channels are rapidly eliminated from the cell surface and targeted for endolysosomal degradation (ELAD) by the endosomal sorting complex required for transport (ESCRT) machinery. Collectively, these results suggest a direct chaperone-independent role of N-glycans in membrane protein energetics and outline a novel paradigm for the metabolic defect of polypeptides with impaired glycosylation in vivo.

Results

Cell surface expression of glycosylation-deficient CFTR is severely reduced

CFTR glycosylation was abolished by mutagenesis of the two consensus Asn-linked N-glycosylation sites (Kornfeld and Kornfeld, 1985) individually (N894D and N900D) or together (2D-CFTR) in CFTR. These mutations decreased the steady-state level of the 3HA-tagged CFTR in both transient (COS-7) and stable (BHK) expression systems as published for untagged CFTR glycosylation mutants (Fig. 1 A and Fig. S1 A; Farinha and Amaral, 2005). The endoglycosidase (endo) H and F sensitivity of N894D- and N900D-CFTR verified that both glycan chains underwent complex glycosylation, whereas the 2D-CFTR failed to obtain N-glycans (Fig. 1 B). Indirect immunostaining of the extracellular 3HA tag in nonpermeabilized cells revealed that N894D-, N900D-, and 2D-CFTR were expressed at the cell surface, as proved by colocalization with Alexa Fluor 594–conjugated wheat germ agglutinine (WGA), a plasma membrane marker (Fig. 1 C). Quantitative analysis of CFTR cell surface density by anti-HA antibody (Ab) binding to the 3HA tag revealed that the N894D-, N900D-, and 2D-CFTR expression level was decreased by ∼37%, ∼63%, and ∼87%, respectively, relative to wild-type (wt) CFTR, which is in line with the immunostaining results (Fig. 1 D). To rule out any specific effect of the 2D substitution, Asn 894 and 900 residues were replaced with Ala (2A-CFTR) and Gln (2Q-CFTR). The cellular and plasma membrane expression of 2A- and 2Q-CFTR was reduced similar to that of 2D-CFTR (Fig. 1, A and D). The 2D-CFTR diminished cell surface expression was consistent with the attenuated cAMP-stimulated iodide efflux (Fig. 1 E). Collectively, these results imply that N-glycans have a substantial role in CFTR biogenesis.

N-glycans enhance CFTR folding efficiency by chaperone-dependent and chaperone-independent mechanisms

The reduction of the glycosylation-deficient CFTR cell surface levels could be attributed to impaired translational rate, ER folding yield, and decreased stability or a combination of these. The translational rates of the glycosylation-deficient and wt CFTR were indistinguishable and measured by the incorporation of [^{35}S]-methionine and [^{35}S]-cystein into CFTR during a short pulse labeling (Fig. S1 B). The limited folding efficiency (30–40%) of the wt CFTR in the ER, conceivably reflecting inefficient post-translational domain assembly (Du et al., 2005; Cui et al., 2007), was monitored by the conversion of the metabolically

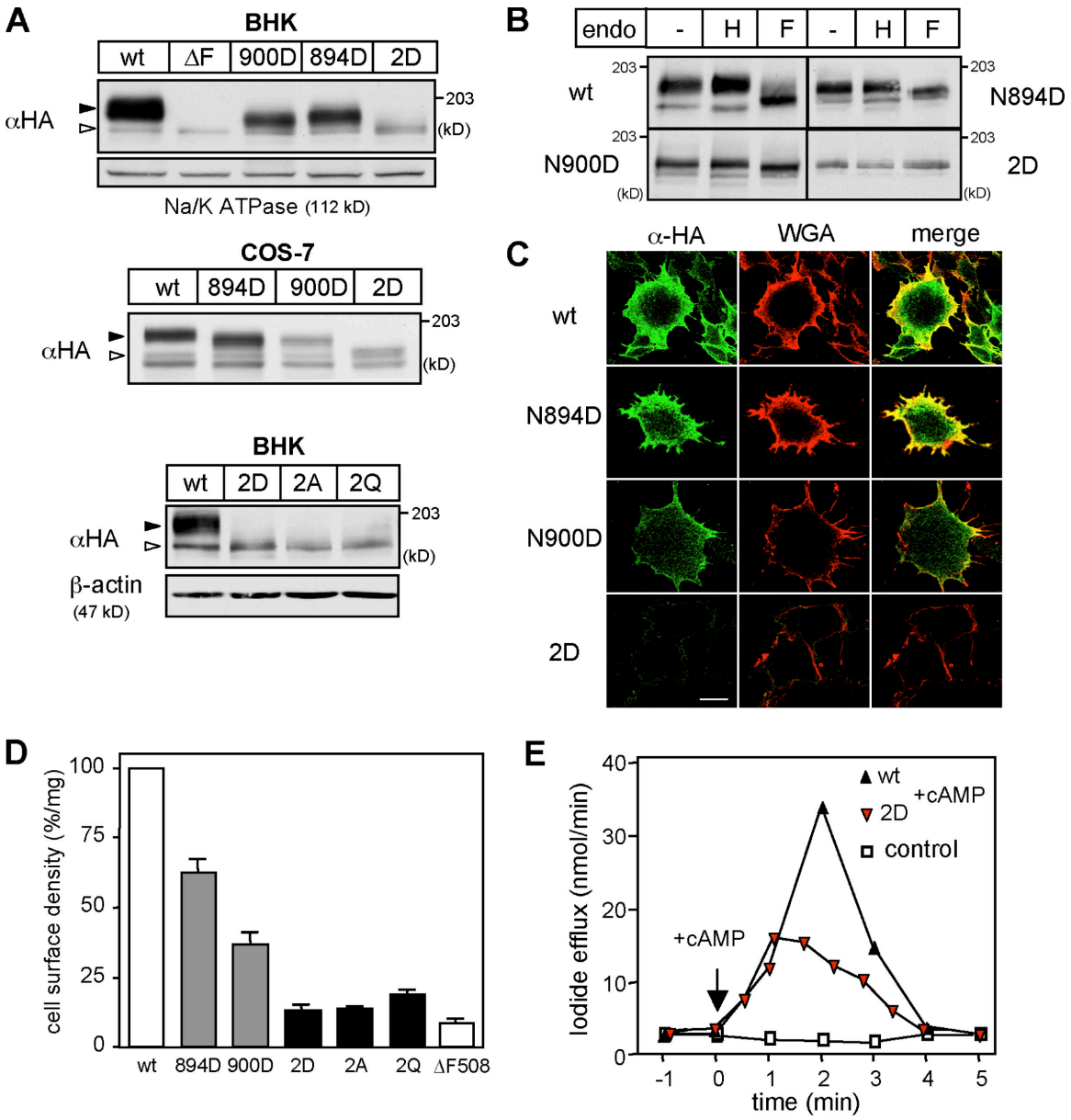

Figure 1. **N-glycosylation defect reduces the cell surface expression of CFTR.** (A) Expression levels of CFTR-3HA variants in stably (BHK) and transiently (COS-7) transfected cells were visualized by immunoblotting. Na^+/K^+-ATPase and β-actin were used as a loading control. Open and closed arrowheads indicate core-glycosylated/nonglycosylated CFTR and complex-glycosylated CFTR, respectively. The ΔF508-CFTR mutant remains core glycosylated. (B) Endo H (H) and PNGase F (F) sensitivity of CFTR variants was assessed by immunoblotting with anti-HA Ab after the incubation of BHK cell lysates with or without endo for 3 h at 33°C. (C) Cell surface expression of CFTR-3HA variants in BHK cells was examined by immunostaining with anti-HA Ab without permeabilization. Plasma membrane was stained with Alexa Fluor 594–WGA. (D) Cell surface density of CFTR variants in BHK cells was measured by anti-HA Ab–binding assay and expressed as a percentage of the wt CFTR normalized for cellular proteins. (E) 2D-CFTR is active in BHK cells, as measured by iodide efflux assay. Error bars indicate mean ± SEM. Bar, 10 μm.

pulse-labeled, core-glycosylated folding intermediates into complex-glycosylated CFTR in the Golgi complex during a 3-h chase. Notably, wt CFTR can achieve its folded protease resistance conformation in the ER without undergoing complex glycosylation upon the inhibition of the ER to Golgi vesicular transport by brefeldin A (BFA; Lukacs et al., 1994; Ward and Kopito, 1994). Both the folded core- and complex-glycosylated channel have a metabolic half-life ≥16 h and are resistant to limited proteolysis in vitro (Lukacs et al., 1994; Zhang et al., 1998). The wt CFTR folding efficiency (34.0 ± 5.6%) was reduced to 15.6 ± 0.5% and 13.8 ± 1.2% in N894D- and N900D-CFTR, respectively (Fig. 2 A).

The 2D-CFTR folding efficiency measurements were based on two observations: (1) elimination of N-glycans accelerated the degradation of the pulse-labeled nonnative wt and did not delay the ΔF508-CFTR removal (Fig. S1, C–E), and (2) the ER expression of the 2D-CFTR was eliminated after 3 h of cycloheximide (CHX) chase, as measured by the colocalization of the 2D-CFTR with CNX (Fig. S1 F). Therefore, the 2D-CFTR folding efficiency could be determined by metabolic pulse-chase experiments after a 3-h chase. The result indicated that only 4.9 ± 1.2% of the newly synthesized 2D-CFTR escaped the ER degradation (Fig. 2 A). Comparable reduction was observed

for 2Q- and 2A-CFTR folding efficiency (Fig. 2 A), implying that the folding defect is not specific to the 2D substitution.

N-glycans may enhance CFTR folding by recruiting lectin-like chaperones and stabilizing folding intermediates and/or by directly altering the folding energetics of the channel (Helenius and Aebi, 2001; Wiseman et al., 2007). To assess the contribution of lectin-like chaperones to CFTR biogenesis, we took advantage of the observation that CNX but not CRT binds to CFTR folding intermediates (Harada et al., 2006; Chang et al., 2008; unpublished data). CNX binding to the core-glycosylated wt and mutant ΔF508-CFTR was prevented by the 2D mutation, which was verified by coimmunoprecipitation (Fig. 2 B). In addition, CNX association with the nonnative core-glycosylated wt and ΔF508-CFTR was also prevented by interfering with monoglucosylated N-glycan formation using the glucosidase inhibitor castanospermine (CAS), confirming previous observations (Pind et al., 1994; Farinha and Amaral, 2005; Rosser et al., 2008; Fig. 2 D, lane 5). Although CAS did not prevent complex glycosylation, 0.1 mM CAS was sufficient to inhibit the α-glucosidase activity in BHK cells by >95% (unpublished data). Obliterating CNX–CFTR interaction by CAS decreased the channel folding only by 30–34% in BHK and HeLa

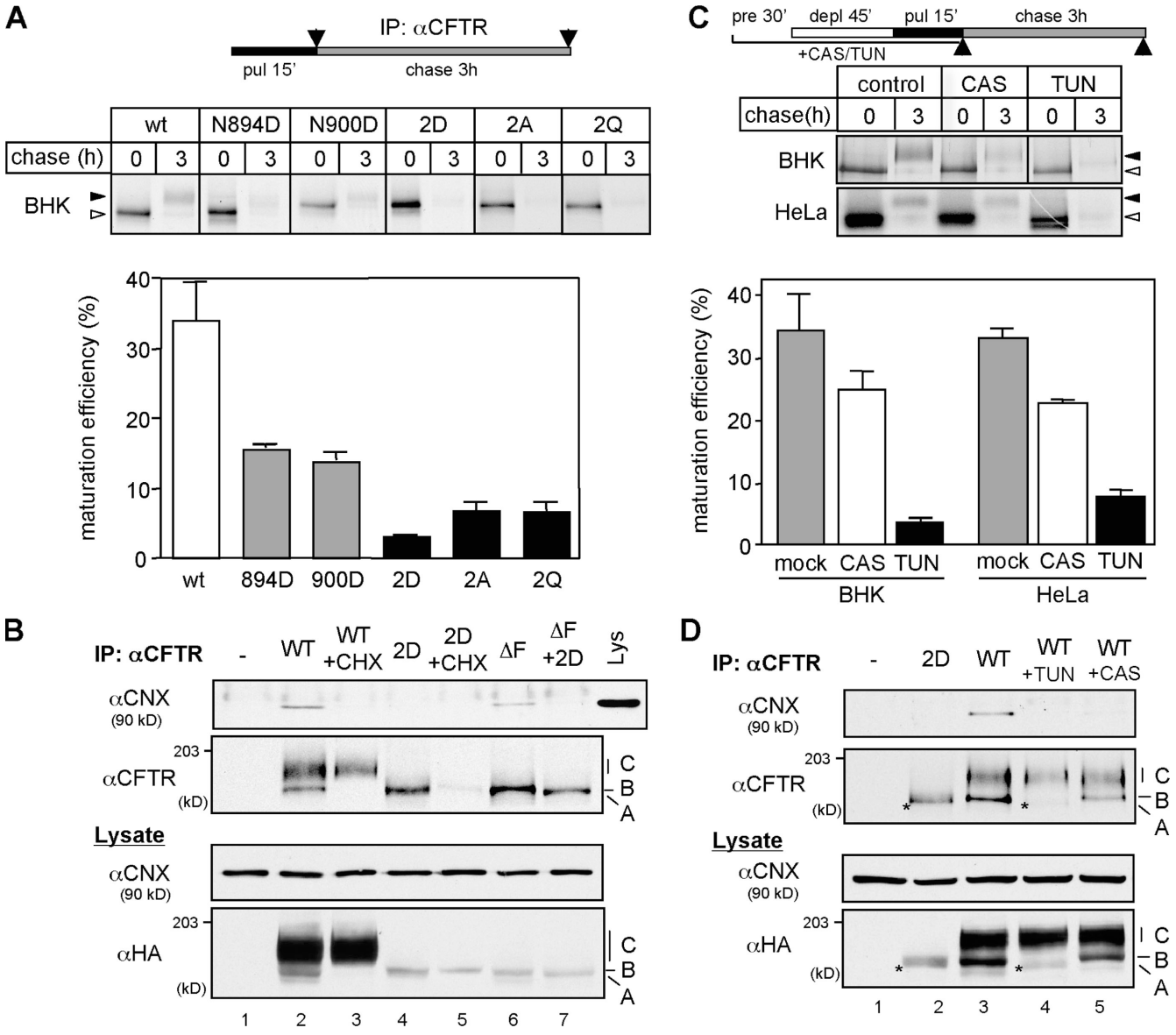

Figure 2. **Defective N-glycosylation severely prevents the productive folding of CFTR.** (A) The pulse-labeled CFTR folding efficiency was determined by the production of the complex-glycosylated form or by the remaining amount of protease resistant (2D) after 3-h chase and expressed as a percentage of the initial radioactivity measured by phosphorimage analysis (n = 3–6). (B) CNX binding to CFTR immunoprecipitates was measured by immunoblotting with anti-CNX Ab. Nonnative folding intermediates (immature form) of wt and 2D-CFTR were eliminated with CHX for 3 h. (C) Differential effect of CAS and TUN on wt CFTR folding efficiency measured as in A in BHK and HeLa cells. Cells were treated with 1 mM CAS or 10 μg/ml TUN for 90 min before and during the pulse labeling (n = 3–5). (D) TUN and CAS treatment (4 h) prevents CNX association with nonnative wt CFTR determined as in B. Asterisks indicate the nonglycosylated wt CFTR. A, B, and C indicate nonglycosylated CFTR, core-glycosylated CFTR, and complex-glycosylated CFTR, respectively. Open and closed arrowheads indicate the core-glycosylated/nonglycosylated CFTR and complex-glycosylated CFTR, respectively. IP, immunoprecipitation; pre, preincubation; deple, depletion; pul, pulse label. Error bars indicate mean ± SEM.

cells (Fig. 2 C). Remarkably, when CNX binding was blocked by an inhibitor of N-glycosylation, tunicamycin (TUN; Fig. 2 D, lane 4), the folding efficiency decreased by 77–84% (Fig. 2 C). The pronounced reduction in the folding efficiency cannot be attributed to TUN-induced unfolded protein response or stress response because the expression levels of Hsp70, BiP, and Grp94 were similar in treated and untreated cells (Fig. S2 A). TUN also failed to impose an ER exit block on the channel, which was measured by immunostaining on CHX-treated cells (unpublished data). Nonspecific effects were minimized by <2-h TUN treatment of cells (Fig. 2 C, top). Assuming complete inhibition of core glycosylation with TUN and CNX binding to CFTR with CAS, these observations imply that ∼45% of the total CFTR folding efficiency (15–16% of the 34%) could be attributed to the direct effect of N-glycans. The comparable folding yield of the 2D-, 2A-, and 2Q-CFTR as well as the TUN-treated wt CFTR support the conclusion that the glycosylation defect is responsible for the severely impaired folding in TUN-treated cells.

To verify the CNX-dependent component of N-glycan function in CFTR folding, HeLa cells were depleted >80% of their CNX content by siRNA (Fig. 3 A). CNX siRNA decreased the CFTR maturation efficiency from 33.8 ± 2.3% to 21.8 ± 1.4% (Fig. 3 B) and the CFTR cell surface expression level by 30% (Fig. 3 C), which were measured by pulse-chase and cell surface Ab binding, respectively. The residual CNX activity cannot account for the limited reduction of CFTR folding efficiency and cell surface density because comparable effects were attained in CAS-treated cells (Fig. 2 C). CNX siRNA did not provoke the up-regulation of Hsp70, Hsp90, BiP, and Grp94 (Fig. 3 A). Furthermore, CFTR expression levels were reduced by a similar extent in mouse embryonic fibroblast derived from the CNX knockout mouse (Okiyoneda et al., 2008). These results, together with our pharmacological and mutagenesis experiments, indicate that N-glycans have a fundamental CNX-independent role in CFTR biogenesis by enhancing its folding efficiency, stabilizing the native fold, or a combination of both.

Core glycans have a permissive role in CFTR stabilization in post-Golgi compartments and at the cell surface

As a surrogate measure of the native-state stability, we examined the metabolic turnover of CFTR variants in post-Golgi compartments. This approach is based on the correlation between the conformational stability and metabolic turnover rates of soluble and membrane proteins including CFTR (Krebs et al., 2004; Sharma et al., 2004; Wiseman et al., 2007). To enhance the radioactive labeling, the pulse duration was extended to 40 min. 3 h of chase was sufficient to eliminate the incompletely folded conformers in the ER (Fig. S1, D and F; and not depicted). The transport-competent native 2D-CFTR has threefold accelerated ($t_{1/2}$ = ∼4 h), whereas the N894D- and N900D-CFTR have approximately twofold faster metabolic turnover rates than the wt channel ($t_{1/2}$ = ∼12 h; Fig. 4, A and B). The turnover of the cell surface 2D-, 2A-, and 2Q-CFTR was accelerated by more than

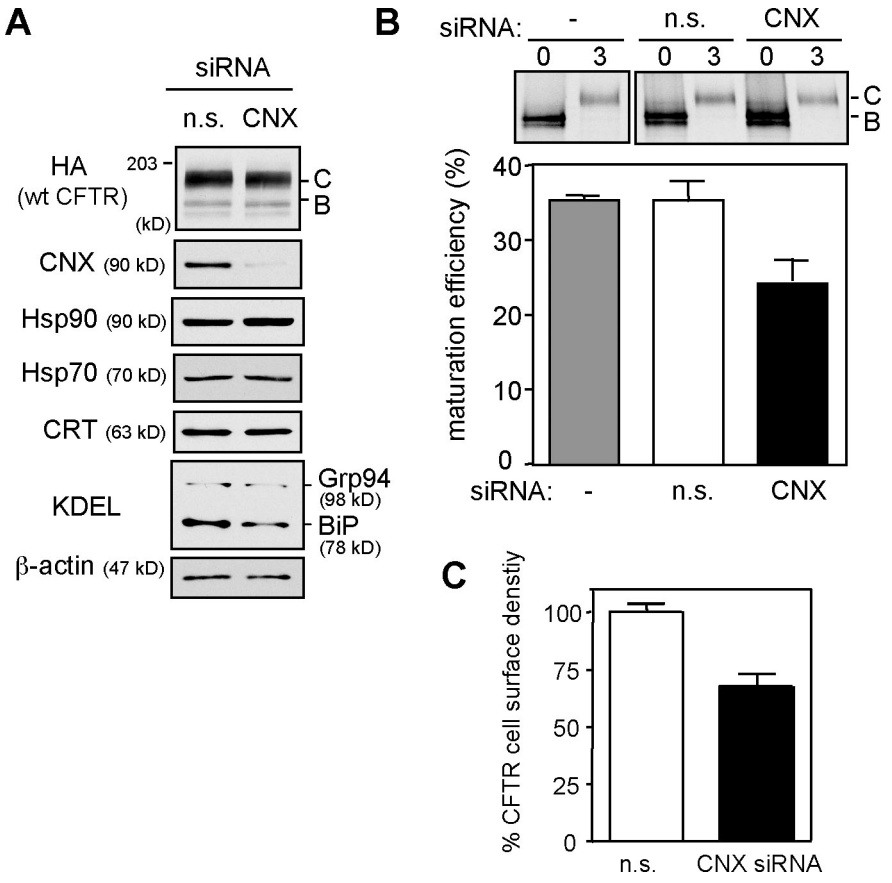

Figure 3. **CNX knockdown partially inhibits CFTR folding.** (A) Selective down-regulation of CNX with 100 nM siRNA in CFTR-expressing HeLa cells. Equal amounts of nonspecific (n.s.) and CNX siRNA–treated lysates were analyzed by immunoblotting. C and B indicate complex-glycosylated CFTR and core-glycosylated CFTR, respectively. (B) Folding yield of wt CFTR in CNX-depleted HeLa cells was measured by pulse-chase experiments (n = 3). (C) Effect of CNX knockdown on the cell surface density of CFTR in HeLa cells (n = 3). Error bars indicate mean ± SEM.

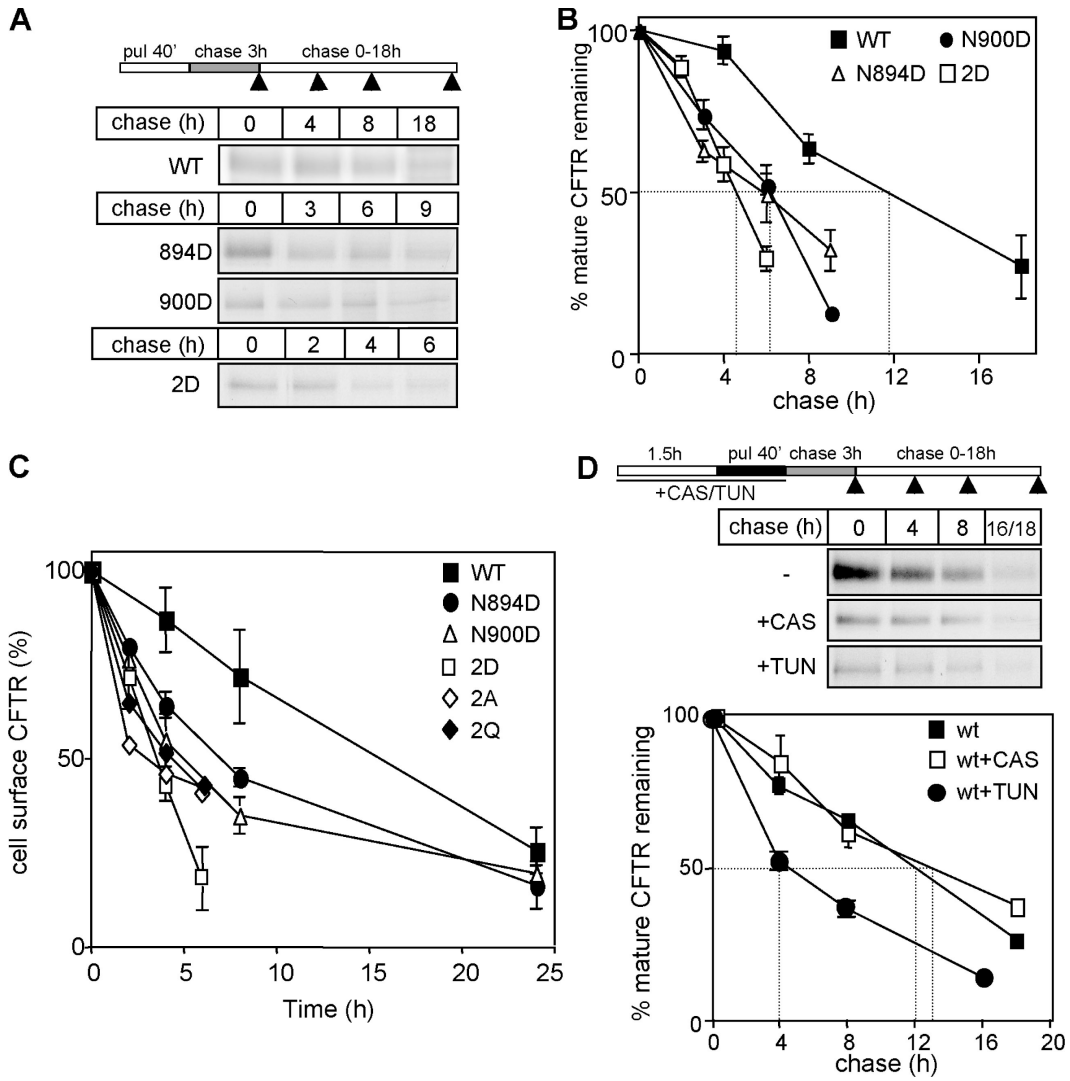

Figure 4. **N-glycans are required for CFTR stability in post-Golgi compartments.** (A and B) Turnover of mature CFTR variants was measured after 40-min pulse labeling (pul) and 3-h chase by immunoprecipitation and phosphorimage analysis ($n = 5$). (C) The cell surface stability of CFTR-3HA variants was determined by anti-HA Ab–binding assay. The disappearance of anti-HA Ab bound to cell surface CFTR was monitored at 37°C ($n = 4$). (D) The effect of TUN and CAS on the turnover of mature wt CFTR in post-Golgi compartments ($n = 3$). Glycosylation inhibitors were present during the preincubation (90 min) and the radioactive pulse (40 min) as indicated. Dashed lines in B and D indicate the half-life of mature CFTR. Arrowheads in the scheme in A and D indicate the time when the sample was collected. Error bars indicate mean ± SEM.

fourfold ($t_{1/2} = \sim 4$ h), which was detected by the disappearance kinetics of the anti-HA Ab–labeled channels in vivo (Fig. 4 C). Importantly, disruption of the CNX–CFTR interaction by CAS and siRNA had no discernable effect on the metabolic and cell surface turnover of the mature CFTR (Fig. 4 D and not depicted). In contrast, TUN, similar to the 2D mutation, destabilized the channel by threefold, supporting the notion that N-glycans are essential determinants of CFTR stability in post-Golgi compartments (Fig. 4 D and not depicted).

As a complementary approach to assess the core-glycosylated CFTR peripheral stability, we used N-acetylglucosaminyl transferase I–deficient HEK293S cells with impaired capacity to synthesize complex-type N-glycans (Reeves et al., 2002). Endo digestion and immunoblotting verified that CFTR underwent only core glycosylation in stably transfected HEK293S cells (Fig. 5, A and B). The core- and complex-glycosylated CFTR exhibited similar expression level and cell surface densities in HEK293S and HEK293 cells, respectively (Fig. 5, A–C). These results imply that core glycosylation is sufficient for the productive folding of CFTR, a conclusion substantiated by the indistinguishable metabolic and cell surface turnover rates of CFTR in HEK293S and control HEK293 cells (Fig. 5, D and E).

N-glycans are not required for CFTR stability after the native fold has been attained

Removal of N-glycan chains has an unpredictable effect on the native fold stability (Wormald and Dwek, 1999; Mitra et al., 2006). Complete deglycosylation of CFTR by recombinant peptide N-glycosidase F (PNGase F) had no discernable effect on the plasma membrane turnover of the wt, 894D-, and 900D-CFTR (Fig. S3, A and B). The CFTR deglycosylation was verified by the channel electrophoretic mobility shift upon in vivo and in vitro endo F treatment (Fig. S3 A). Similar results were

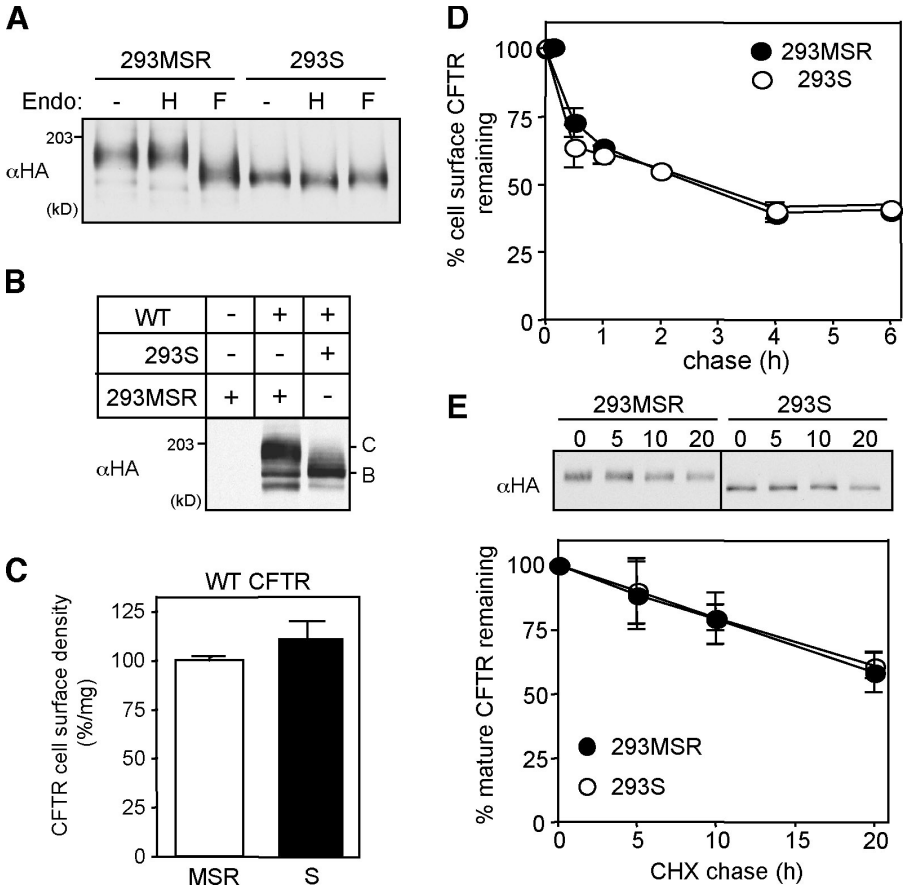

Figure 5. **Core glycosylation is sufficient for the folding and stability of CFTR.** (A) Endo H (H) and PNGase F (F) sensitivity of wt CFTR in HEK293S cells was assessed by immunoblotting with anti-HA Ab after the incubation of cell lysates for 3 h at 33°C. HEK293MSR cells were used as control. Steady-state level (B) and cell surface density (C) of wt CFTR in HEK293S cells (n = 3). (D) Cell surface stability of wt CFTR in HEK293S cells was measured by anti-HA–binding assay (n = 3). MSR and S indicate HEK293MSR and HEK293S cells, respectively. C and B indicate complex-glycosylated CFTR and core-glycosylated CFTR, respectively. (E) Turnover rates of the mature complex-glycosylated CFTR and core-glycosylated CFTR in HEK293MSR and HEK293S cells, respectively. Metabolic turnover of CFTR was measured by CHX chase after an initial CHX treatment (3 h) to eliminate the ER resident folding intermediates (n = 3). Error bars indicate mean ± SEM.

obtained by the cleavage of high mannose-type oligosaccharides (core glycans) of the cell surface resident CFTR using recombinant endo A (endo-β-*N*-acetylglucosaminidase in HEK293S cells; Fig. S3 C; Fan et al., 1995). Thus, neither the core nor the complex glycans are necessary to maintain the CFTR native fold once it was attained similar to a subset of glycoprotein (Cronin et al., 2005; daCosta et al., 2005).

Defective endocytic recycling accounts for the premature degradation of the glycosylation-deficient CFTR from the cell surface

To assess the role of internalization in the accelerated turnover of glycan-deficient CFTRs, the channel endocytosis rate was determined by the anti-HA Ab uptake assay. The internalization rates of the glycosylation-deficient and wt CFTR were similar (Fig. 6 A). In contrast, the recycling of 894D- and 900D-CFTR was inhibited by 50–60%, whereas the 2D-CFTR was inhibited by >80% during a 10-min chase (Fig. 6 B). CFTR recycling was measured by monitoring the reappearance of biotinylated Ab–CFTR complex from the endosomal compartment with NeutrAvidin-HRP, as described in Materials and methods. The severely impeded recycling may account for the rapid metabolic turnover of the 2D-CFTR at plasma membrane. In support of this inference, although the wt CFTR avoided lysosomal delivery, the glycosylation mutants accumulated in dextran-labeled lysosomes (Fig. 6 C). As a corollary, the internalized wt but not the glycosylation mutant was confined to transferrin-labeled recycling endosomes (Fig. 6 C).

The distinct destination of internalized wt and mutant channels was substantiated by monitoring the postendocytic sorting of FITC-labeled channel using vesicular pH (pH_v) measurements of CFTR-containing vesicles with fluorescence ratiometric image analysis (FRIA; Sharma et al., 2004; Barriere et al., 2007). After the internalization of anti-HA Ab and FITC-conjugated Fab secondary Ab complexed with CFTR for 1 h, cells were chased in Ab-free medium for 30 min. FRIA confirmed that wt CFTR was excluded from lysosomes and confined, predominantly, to the mildly acidic (pH 6.4 ± 0.01) recycling endosomal compartment both in control and CNX-depleted cells (Fig. 6 D and not depicted). Similar results were obtained on wt CFTR harboring only core oligosaccharides in HEK293S cells (Fig. 6 E). In sharp contrast, internalized 2D-CFTR, and to a lesser extent the 894D- and 900D-CFTR, were excluded from recycling endosomes and targeted into more acidic late endosomes and multivesicular body (MVB)/lysosomes displaying mean pH_v of 4.9–5.5 (Fig. 6, D and E). Considering that the anti-HA Ab dissociation at pH = 5 is negligible from the CFTR-3HA (Kumar et al., 2007), both the pH measurements and the immunolocalization data demonstrate that the glycosylation-deficient CFTRs are preferentially targeted to MVB/lysosomes.

Ub-dependent endosomal sorting machinery is involved in the lysosomal targeting of the 2D-CFTR

We have previously shown that CF-causing mutations residing in the cytosolic domains (e.g., ΔF508) are associated with

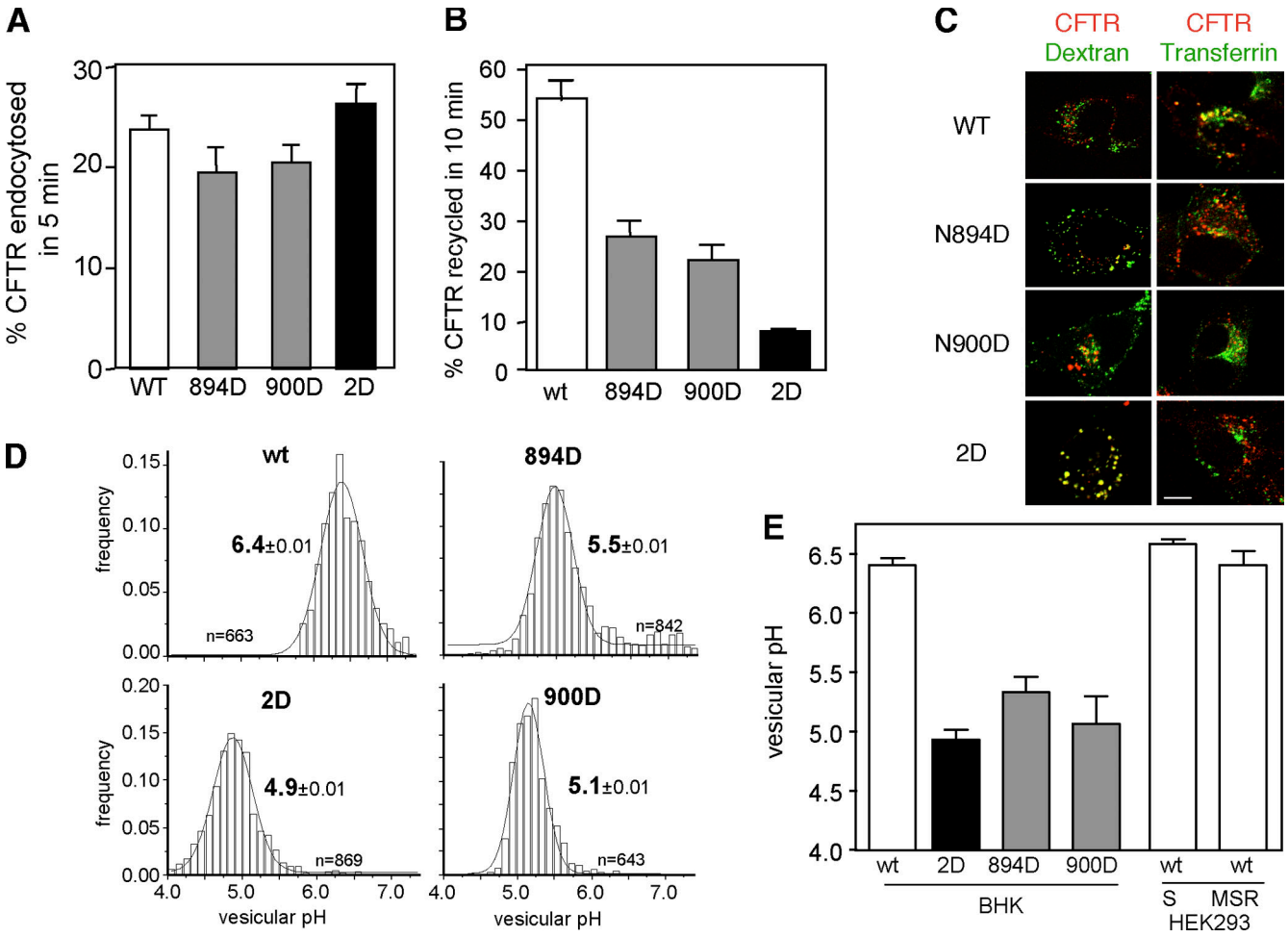

Figure 6. **Lysosomal targeting and inefficient endocytic recycling account for the cell surface instability of glycosylation-deficient CFTR.** (A) Internalization rate of CFTR variants in BHK cells was measured by anti-HA Ab uptake assay as described in Materials and methods (n = 3–6). (B) Endocytic recycling of CFTR variants in BHK cells was measured by the biotin-NeutrAvidin sandwich assay as described in Materials and methods (n = 3). (C) Colocalization of internalized CFTR with FITC-dextran–loaded lysosomes and FITC-transferrin–labeled early endosomes was analyzed by laser confocal microscopy as described in Materials and methods. CFTR variants were internalized with anti-HA Ab complexed to TRITC-conjugated anti–mouse IgG or Fab for 1 h at 37°C and chased in Ab-free medium for 30 min. Single optical sections obtained by laser confocal microscopy were taken, and only overlay images are shown. (D) The pH of the endocytic vesicles containing CFTR variants was measured by single-cell fluorescence ratio image analysis using in situ calibration curve. The pH of >300 vesicles was determined in each experiment as described in Materials and methods. (E) The mean pH of vesicular populations containing internalized CFTR variants in BHK, HEK293MSR (MSR), and HEK293S (S) cells from 3–4 independent experiments. Error bars indicate mean ± SEM. Bar, 10 µm.

conformational defects and increased ubiquitination of CFTR in post-Golgi compartments (Sharma et al., 2004). Although N-glycans are localized on the exofacial surface, we hypothesized that the conformational defect imparted by glycan deficiency may be relayed to the cytosolic domains and provokes ubiquitination of the channel. The following evidence suggests that this is indeed the case.

(a) The normalized ubiquitination level of the 2D-CFTR in post-Golgi compartments was approximately fivefold higher than wt CFTR, which was demonstrated by denaturing immunoprecipitation and anti-Ub immunoblotting of CFTR (Fig. 7, A and B). The immature, ER-associated ubiquitinated form of CFTR was eliminated by CHX treatment for 3 h before immunoprecipitation.

(b) Both the cell surface turnover rate and the lysosomal targeting of the 2D-CFTR was delayed after the inhibition of the ubiquitination machinery by ablating the thermosensitive E1 Ub-activating enzyme in ts20 but not in the parental E36 CHO cells at 40°C (Fig. 7, C and D). The down-regulation of the E1 enzyme was verified by immunoblotting (Fig. 7 C, inset). After the E1 enzyme down-regulation in ts20 but not in E36 cells, internalized 2D-CFTRs were predominantly associated with recycling endosomes based on the pH_v determination by FRIA (Fig. 7 D). This implies that the lysosomal targeting of the 2D-CFTR was dependent on the E1 enzyme activity.

(c) Consistent with the notion that ubiquitination plays a critical role in the lysosomal targeting of the 2D-CFTR, depletion of cellular Hrs (hepatocyte growth factor–regulated tyrosine kinase substrate) and TSG101, Ub-binding proteins of the ESCRT-0 and -I complexes, respectively, with an established role in the lysosomal sorting of ubiquitinated cargoes (Slagsvold et al., 2006; Saksena et al., 2007), impeded the 2D-CFTR but not Lamp1 lysosomal delivery (Fig. 7, E and F; and not depicted). The efficiency of the siRNA was verified by immunoblotting (Fig. 7 E). The lack of

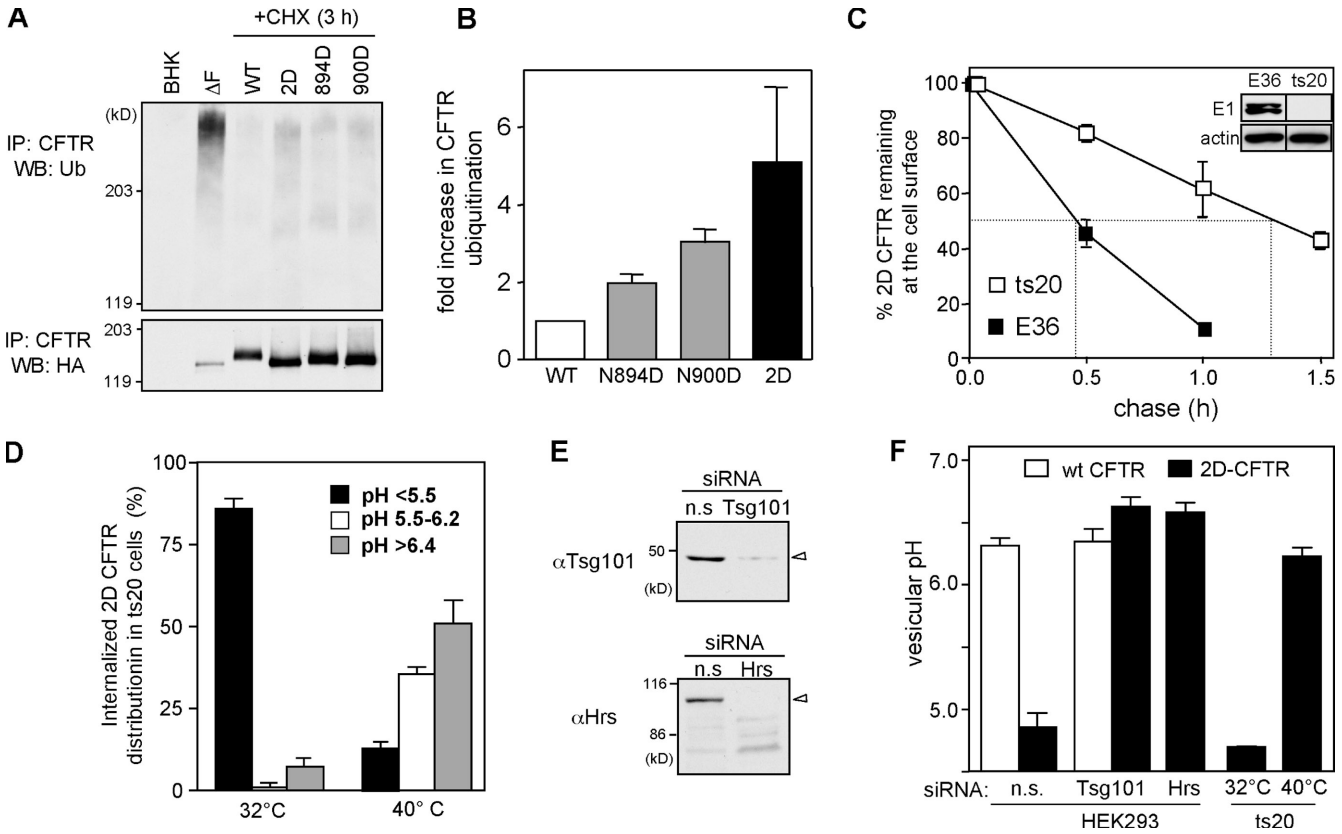

Figure 7. **Ubiquitination acts as sorting signal directing glycosylation-deficient CFTR into lysosome.** (A) Ubiquitination level of CFTR variants in post-Golgi compartments of BHK cells was measured by denaturing immunoprecipitation (IP) and immunoblotting with anti-Ub Ab. Five- to sixfold more cells were used for the glycosylation-deficient CFTR isolation. Protein loading was adjusted to have a comparable amount of wt and glycosylation-deficient CFTR. (B) Relative ubiquitination was measured by densitometry after normalization for the amount of precipitated CFTR. (C) Cell surface stability of 2D-CFTR in ts20 and E36 cells was measured by anti-HA Ab binding. Cells were exposed to 40°C for 2.5 h to inactive E1, as verified by immunoblotting (inset). Dashed lines in the plot indicate the half-life of cell surface CFTR. (D) The pH of the endocytic vesicles containing 2D-CFTR in ts20 cells preincubated at 32 or 40°C for 2.5 h was measured at 37°C by FRIA. The percentage of 2D-CFTR residing in vesicles with the indicated pH is plotted. (E) Down-regulation of Hrs and TSG101 by siRNA was verified in HEK cells by immunoblotting. Equal amounts of proteins were loaded. (F) The mean pH of vesicles containing wt or 2D-CFTR variants in HEK cells transfected with 50 nM TSG101, Hrs, or nonspecific (n.s.) siRNA as described in Materials and methods. Sorting of 2D-CFTR in ts20 cells preincubated at 32 or 40°C for 2.5 h was measured by FRIA (n = 3). WB, Western blot. Error bars indicate mean ± SEM.

off-target effects of siRNA was confirmed by the preserved recycling of wt CFTR and by the distinct postendocytic destination of 2D-CFTR in the presence of nonspecific siRNA (Fig. 7 F). Collectively, these results are consistent with the notion that N-glycans can stabilize the channel native fold and therefore prevent its premature ubiquitination in post-Golgi compartments.

Conformational destabilization of CFTR in the absence of N-glycosylation

To assess the N-glycan–induced structural changes, we compared the protease susceptibility of the wt and 2D-CFTR in their native environment, which is a method used previously to unravel conformational differences in CFTR cytosolic domains (Zhang et al., 1998). Immunoblotting showed that the proteolytic digestion patterns of the native core-glycosylated (ER retained form by BFA) and complex-glycosylated wt CFTR were identical, whereas they substantially differed from the wt core-glycosylated folding intermediates and misfolded ΔF508-CFTR (Zhang et al., 1998; Du et al., 2005).

For selective probing the mature wt and 2D-CFTR conformers, the ER-associated folding intermediates were eliminated by exposing the BHK cells to CHX for 3 h before microsomes were isolated by differential centrifugation. The global trypsin and chymotrypsin resistance of the full-length 2D-CFTR (~160 kD) was decreased as compared with wt CFTR (~190 kD; Fig. 8, left). A 50% loss of the mature 2D-CFTR was achieved at a 10-fold lower trypsin concentration (Fig. S4 B).

The protease resistance of the four major domain-containing fragments (MSD1 [1–388 aa], ~45 kD; NBD1 [389–678 aa], ~29 kD; MSD2 [837–1,178 aa], ~39 kD; and NBD2 [1,152–1,440 aa], ~29 kD; the predicted molecular mass of the domain is indicated) generated by limited proteolysis was examined with domain-specific antibodies MM13-4, 660, HA, and M3A7, respectively (Cui et al., 2007). Modest or no significant reduction was observed in the trypsin resistance of NBD1 and NBD2 fragments as well as in the MSD1. Comparison of the wt and 2D MSD2 (~75–80 and 50 kD) indicated a significant decrease in protease resistance of the 2D-CFTR by the appearance of immunoreactive degradation intermediates (~38 and ~24 kD; Fig. 8, left, asterisks) at a high trypsin concentration (Fig. 8, left). To avoid the complex glycosylation of the wt CFTR, limited proteolysis was also performed on wt- and 2D-CFTR–expressing cells

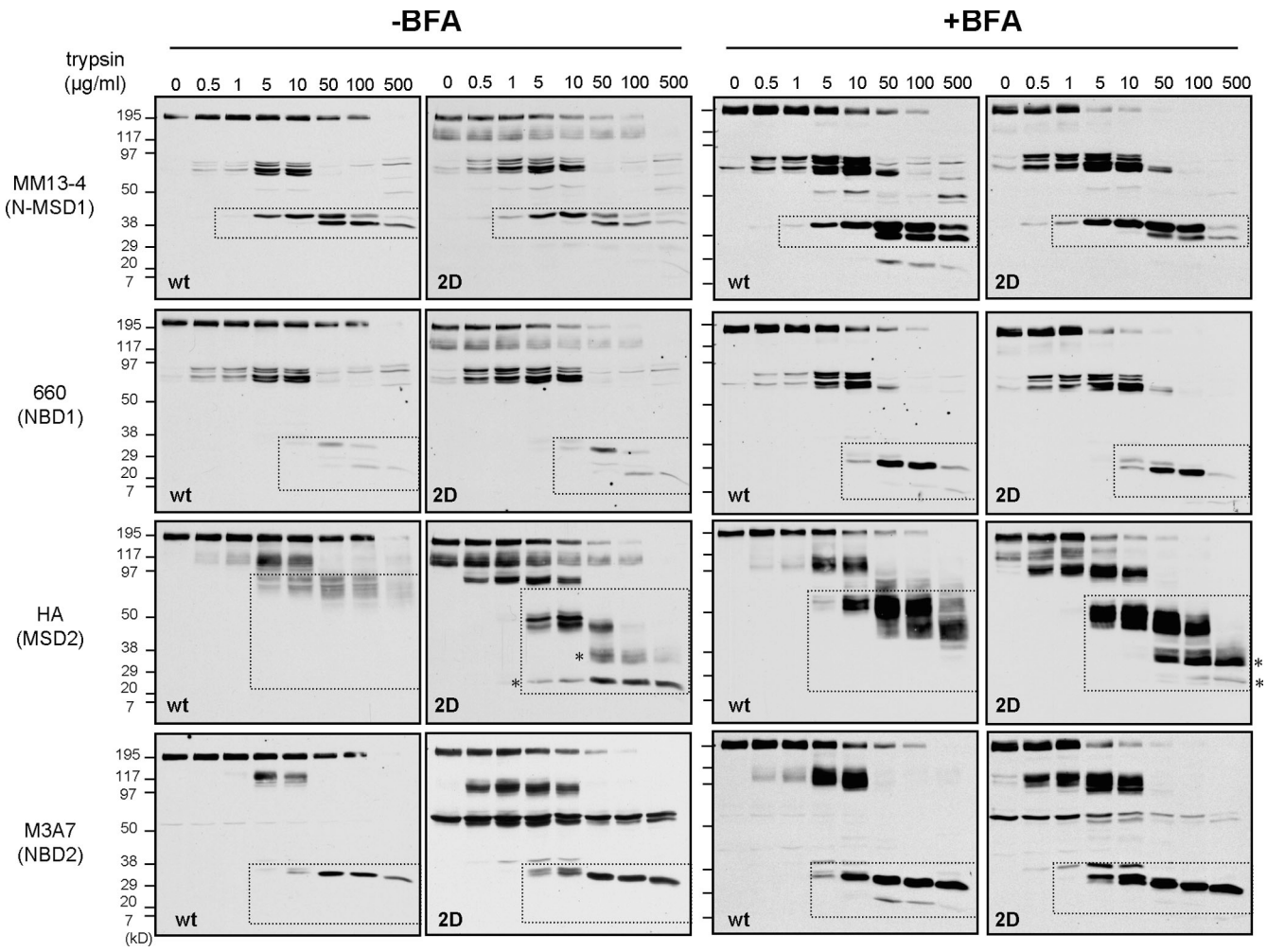

Figure 8. **N-glycosylation increases the protease resistance of the mature CFTR.** Limited trypsinolysis of the wt and 2D-CFTR. Isolated microsomes from BHK cells treated with or without 5 μg/ml BFA for 24 h were exposed to trypsin. Proteolytic patterns were visualized by immunoblotting with domain-specific (shown in parentheses) anti-CFTR antibodies. Dashed regions designate putative fragments containing the Ab-specific domains validated previously (Du et al., 2005; Cui et al., 2007). The glycosylation defect provoked increased protease susceptibility of the MSD2 relative to wt in the absence as well as in the presence of BFA. The asterisks designate novel MSD2 degradation intermediate in the 2D-CFTR.

treated for 24 h with BFA and CHX during the last 3 h. This protocol ensured the accumulation folded wt and 2D-CFTR and the elimination of the unfolded wt and 2D-CFTR at the ER. The differential protease susceptibility of the MSD2 fragment of the wt and 2D-CFTR was confirmed on BFA-treated cells (Fig. 8, right). The nonglycosylated 2D but not the wt MSD2 (~52–55 kD) was cleaved into ~35- and ~24-kD fragments (Fig. 8, right, asterisks). Similar results were obtained by chymotrypsin digestion (Fig. S4 A). Collectively, these results rule out that heterogeneity in plasma membrane vesicles orientation or the exposure of a single cleavage site provoked the differential protease susceptibility of the 2D-CFTR.

The 2D-CFTR increased thermoaggregation propensity provided supporting evidence for the conclusion that N-glycans contribute to the thermal stability of CFTR. The thermoaggregation tendency of CFTR was measured by determining the aggregation-resistant fraction of the SDS-solubilized monomeric channel after thermodenaturation at 37–100°C (Sharma et al., 2001). To eliminate the contribution of the ER-associated folding intermediates, cells were exposed to CHX for 3 h before microsome isolation. 50% of solubilized 2D-CFTR was aggregated at an ~10°C lower temperature than its wt counterpart (Fig. 9, A and B), a phenomenon also observed for the structurally destabilized ΔF508-CFTR (Sharma et al., 2001). The differential thermoaggregation appears to be an indicator of the remaining secondary structure of detergent-solubilized CFTR considering that the difference was eliminated in 8 M urea, and the aggregation propensities of Grp78 and the Na^+/K^+-ATPase were comparable in the two CFTR-expressing cell lines (Fig. 9 A and not depicted). Finally, we also showed that the cellular and cell surface expression of the glycosylation mutants is temperature sensitive, similar to the metabolic turnover of the 2D-CFTR (Fig. 9, C and D; and not depicted).

Discussion

Our results provide direct evidence for the dual role of N-glycan as a chaperone-dependent and -independent promoter of CFTR biogenesis and represent one of the first attempts to understand the consequence of N-glycosylation on a polytopic membrane

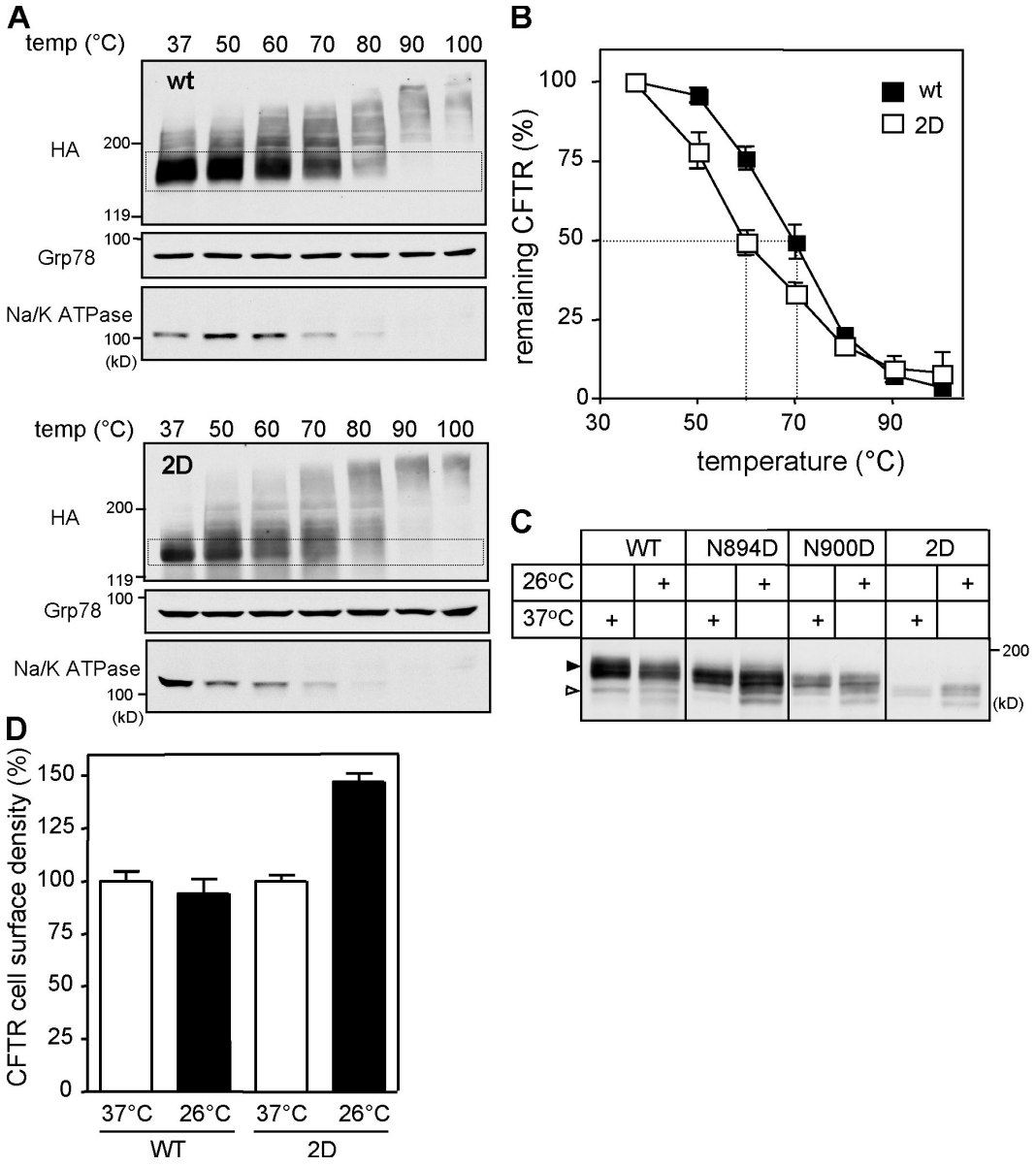

Figure 9. **N-glycosylation enhances the thermal stability of CFTR.** (A and B) Determination of the mature wt and 2D-CFTR thermoaggregation propensity. wt (top) and 2D-CFTR (bottom) were solubilized in RIPA buffer after CHX treatment of the cells for 3 h. Cell lysates were mixed with LSB and incubated at the indicated temperature for 5 min. Aggregates were pelleted by centrifugation, and soluble fractions were analyzed with immunoblotting. Dashed regions indicate the monomeric mature form of wt and 2D-CFTR. (B) The monomeric wt and 2D-CFTR were quantified with densitometry on immunoblots shown in A and expressed as the percentage of the amount detected at 37°C incubation ($n = 3$). (C and D) The effect of low temperature (26°C for 24 h) incubation on the steady-state level (C) and cell surface density (D) of 2D-CFTR, as measured by Western blotting and anti-HA Ab binding, respectively ($n = 3$). Open and closed arrowheads indicate the core-glycosylated/nonglycosylated and complex-glycosylated CFTR, respectively. Error bars indicate mean ± SEM.

protein folding energetics in vivo. Although CNX binding increased the CFTR folding efficiency, only glycan modification could influence the native-state structural stability. Based on the increased ubiquitination and distinct post-Golgi trafficking, we outline some of the critical steps in the cellular and molecular mechanisms responsible for the cell surface stability defect of the glycan-deficient CFTR.

The direct chaperone-independent role of N-glycans in CFTR folding and stability

In addition to the well-established role of N-glycans as a molecular signal for CNX recruitment to CFTR (Pind et al., 1994; Okiyoneda et al., 2004, 2008; Farinha and Amaral, 2005; Chang et al., 2008), we show in this study that N-linked oligosaccharides have an intrinsic ability to enhance the nascent CFTR folding and native-state stability similar to that observed in a subset of soluble protein in vitro (Imperiali and O'Connor, 1999; Wormald and Dwek, 1999; Mitra et al., 2006). Considering the extent of CNX inactivation and glycosylation inhibition on CFTR folding efficiency, the direct and indirect (CNX dependent) impact of N-glycans appears to be comparable. Although we cannot preclude the possibility that the effect could be partially a result of interactions between core glycans of CFTR and other cellular factors, this may be

minimal because CAS treatment and CNX knockdown had comparable impact on the folding efficiency. These results suggest that evolutionary acquisition of N-glycans could serve to optimize the folding energetics independently of the CNX/CRT folding cycle without imposing significant alteration in the polypeptide amino acid sequence and function in both soluble and integral membrane proteins.

Although the modestly decreased (~35%) folding efficiency in the absence of CNX interaction confirms previous studies (Farinha and Amaral, 2005; Okiyoneda et al., 2008; Rosser et al., 2008), the accelerated posttranslational folding kinetics of CFTR have not been demonstrated yet (Fig. S2 B). This latter phenomenon could be explained by the CNX-induced stabilization of MSD2 and protection against premature ERAD (Rosser et al., 2008), which is similar to the stabilization of α1-antitrypsin null Hong Kong mutant by CNX (Oda et al., 2003). Chaperone-mediated stabilization of soluble folding intermediates has been observed at the single molecule level (Bechtluft et al., 2007) and in population both in vitro and in vivo (Agashe et al., 2004).

How can we envision the N-glycan folding effect on CFTR? In addition to localized conformational change in the MSD2 (Rosser et al., 2008), N-glycans may alter the global stability of CFTR, displaying extensive domain–domain interactions (Du et al., 2005; Cui et al., 2007; Serohijos et al., 2008). Localized structural changes are reflected by the protease hypersensitivity of the glycan-deficient MSD2-containing fragment and suggested by the decreased cell surface expression of the transmembrane segment 7-8 hairpin in the absence of glycosylation (unpublished data). The global conformational defect is supported by the increased thermoaggregation and protease susceptibility of the full-length mature 2D-CFTR regardless of whether it is confined to the ER or post-Golgi compartments (Figs. 8 and 9 and Fig. S4). Furthermore, the increased ubiquitination, as well as the decreased cell surface stability, provided indirect evidence for the cellular manifestations of the 2D-CFTR structural instability.

Localized induction of β turn and infrequently β strand by interaction between the N-acetyl group of the first GlcNAcs and soluble polypeptide has been documented (O'Connor and Imperiali, 1996). N-glycans could also enhance the refolding propensity and stability of several globular polypeptides (Mitra et al., 2006). Thermal stabilization of engineered SH3 domain variants after polysaccharide chain conjugation was demonstrated by the molecular dynamics study (Shental-Bechor and Levy, 2008). Interestingly, the stabilization effect was dependent on the position of the glycans but only very weakly on its size. Collectively, based on these and other observations (Helenius and Aebi, 2004), it is conceivable that N-glycans limit the conformational space accessible to the transmembrane segments, facilitating posttranslational CFTR domain folding. In accord, with the localized effect of the glycan chain, partial reversion of the expression and folding defect of the 900D- and 2D-CFTR was observed by introducing a validated glycosylation site (T908N) in the fourth extracellular loop (Hammerle et al., 2000; Fig. S5).

Although cotranslational glycosylation conceivably exerts a profolding change in the energy landscape of CFTR, N-glycans are not involved in maintaining the native-state stability once it has been attained. This is not surprising because deglycosylation of a subset of soluble and membrane proteins had no impact on their thermodynamic and metabolic stabilities (Cronin et al., 2005; daCosta et al., 2005; Mitra et al., 2006).

It is recognized that N-glycan participates in the ER quality control by ensuring lectin chaperone-mediated ER retention and ERAD (Helenius and Aebi, 2004; Molinari, 2007). Intriguingly, a lack of N-glycans did not influence the ER retention of unfolded CFTR (Fig. S1 E), which is consistent with a recent study (Chang et al., 2008). Although CNX and Man_8-specific EDEMs are required for the ERAD of several misfolded polypeptides, CNX knockout (Okiyoneda et al., 2008) and glycosylation defect stimulated the nonnative wt CFTR channel elimination (Fig. S1, C and D). This suggests that alternative recognition mechanisms (e.g., recruitment of the Hsp70/Hsc70-CHIP-UbcH5, Rma1-Ubc6, and gp78) are involved in wt CFTR ERAD (Meacham et al., 2001; Younger et al., 2006; Morito et al., 2008). In contrast, 2D mutation failed to delay the ΔF508-CFTR the ERAD kinetics (Fig. S1 E), implying that N-glycans have minimal stabilizing effect on the mutant CFTR.

The cellular and molecular basis of the glycan-deficient CFTR instability at the plasma membrane

We have shown that the glycan-deficient 2D-CFTR has severalfold decreased metabolic and cell surface stability similar to the replacement of Asn residues with Ala and Gln in the consensus glycosylation sites consistent with earlier results (Farinha and Amaral, 2005). This observation rules out the possibility that the Asp residue substitutions by itself account for the mutant phenotype. We believe that localized unfolding of the glycan-deficient channel initiates the recruitment of the cytosolic chaperone Ub system, leading to Ub conjugation and targeting the channel for proteolysis by the ELAD as part of the peripheral protein quality control mechanism to preserve proteostasis (Sharma et al., 2004; Balch et al., 2008). The severely inhibited recycling at normal internalization rates as well as the preserved metabolic stability of the core-glycosylated and -deglycosylated CFTR implies that the cell surface retention of the native channel is independent of galectin-glycoprotein lattice formation, contrary to the regulation of other receptors (e.g., EGF receptor) and transporters (e.g., GLUT2; Lau et al., 2007).

Considering that Ub has been identified as an internalization and a MVB/lysosomal sorting signal (Raiborg et al., 2003; Traub and Lukacs, 2007), it is reasonable to assume that ubiquitination is the predominant signal for the glycan-deficient CFTR ELAD, although the role of additional pathways cannot be ruled out. The role of Ub conjugation in the structurally unstable 2D-CFTR turnover is supported by its fivefold increased ubiquitination relative to its wt counterpart in post-Golgi compartments, as well as its greater than threefold slower turnover at the cell surface upon inactivation of the ubiquitination machinery. Consistently, Ub-binding endosomal sorting adaptors, Hrs, similar to the TSG101, were found to be functionally indispensable in the MVB/lysosomal delivery of the 2D-CFTR by rerouting it from constitutive recycling. Although constituents of the ESCRT0-III have been established to mediate

MVB/lysosomal sorting of plasma membrane proteins (e.g., EGF receptor) after ligand/signal-dependent ubiquitination (Raiborg et al., 2003; Slagsvold et al., 2006), the function of the ESCRT in the quality control of endocytic cargo is less well described. The accelerated cell surface turnover in concert with the lysosomal targeting of the 2D-CFTR provides a second example that is reminiscent of nonnative ΔF508- and Δ70-CFTR degradation from the cell surface. Both mutants, but not the wt CFTR, were found to physically associate with Hrs, STAM, TSG101, Vps25, and Vps32, components of the ESCRT0-III, although the functional significance of these interactions in the mutant lysosomal sorting has not been examined yet (Sharma et al., 2004).

Besides elucidating the complex role of N-glycans in CFTR biogenesis, our observations have two important implications. First, they emphasize that N-glycans also influence the ELAD kinetics from the plasma membrane. This conclusion supports the hypothesis that folding energetic is a critical determinant of membrane protein turnover not only at the early secretory pathway (Wiseman et al., 2007) but at the post-Golgi endosomal axis as well (Sharma et al., 2001, 2004; Arvan et al., 2002; Krebs et al., 2004). The 2D-, ΔF508- and Δ70-CFTR conformational destabilization correlates with their ubiquitination, metabolic destabilization, and preferential MVB/lysosomal targeting from the cell surface, representing key events in a complex quality control mechanism for integral plasma membrane proteins in mammalian cells. Second, the aforementioned proposed paradigm of the 2D-CFTR degradation may serve as a testable model for the accelerated turnover of several glycosylation-deficient plasma membrane proteins, e.g., aquaporin-2, H^+/K^+-ATPase β subunit, ABCB11, rhodopsin, dopamine D2 receptor, GLUT1, and β-adrenergic receptor, caused by presently unknown mechanisms (Rands et al., 1990; Asano et al., 1993; Hendriks et al., 2004; Vagin et al., 2004; Watanabe et al., 2004; Zhu et al., 2004; Mitra et al., 2006; Free et al., 2007; Mochizuki et al., 2007).

Materials and methods

Recombinant DNA constructs

Asn residues at positions 894 and 900 in the two consensus N-glycosylation sites of CFTR were replaced with Asp, Ala, or Gln residues using overlapping PCR. The PCR products were introduced into pNut-wt-CFTR-3HA construct using BspEI/PmlI restriction sites. The N894D-/N900D-CFTR (2D-CFTR) was generated using the N894D-CFTR as a template and the N900D mutagenic primers. Similar strategy was used to generate N900D+T908N- and 2D+T908N-CFTR constructs. ΔF508-CFTR-3HA containing the 2D mutations was generated by PCR mutagenesis.

Cell culture and transfection

Stably transfected BHK cell lines expressing wt, N894D, N900D, 2D-, 2A-, and 2Q- or ΔF508-CFTR-2D as well as N900D+T908N- and 2D+T908N-CFTR variants were generated as described previously (Du et al., 2005). After selection, 50–100 methotrexate-resistant clones were pooled and expanded for experiments. Experiments were performed on 3HA-tagged CFTR variants if not indicated otherwise. E36 and ts20 CHO cell lines stably expressing the wt and 2D-CFTR were generated by retroviral infection as described previously (Benharouga et al., 2003). HEK293S cells were provided by G. Khorana (Massachusetts Institute of Technology, Cambridge, MA). Transient expression of CFTR variants in COS-7 cells was accomplished using the FuGENETM6 reagent (Roche). HeLa cells stably expressing wt CFTR-3HA were generated by lentiviral infection by J. Wakefield (Tranzyme, Durham, NC). CAS was purchased from Toronto Research Chemicals, and TUN was purchased from Sigma-Aldrich.

Electrophoresis and immunoblotting

Immunoblotting was performed as described previously (Sharma et al., 2004). The following antibodies were used: HA (HA.11), Myc (9E10), E1 Ub-activating enzyme (Covance), and CFTR. M3A7 Ab was mapped to the C-terminal region of NBD2 (1,375–1,383 LDPVTYQIIR residues), and the 660 Ab, provided by J. Riordan (University of North Carolina at Chapel Hill, Chapel Hill, NC), recognizes the core of NBD1 (Cui et al., 2007). Ub (P4D1; Santa Cruz Biotechnology, Inc.), Na^+/K^+ ATPase Ab (a6F; Developmental Studies Hybridoma Bank), CNX (SPA860), CRT (SPA600), Hsc70 (C92F3A-5), KDEL (10C3; Assay Designs), and β-actin (ab8226; Abcam) were also used.

Metabolic pulse-chase experiments

CFTR turnover was measured by metabolic pulse-chase experiments essentially as described previously (Lukacs et al., 1994). The pulse labeling duration was 15 min if not indicated otherwise.

Cell surface density measurements and internalization of CFTR

The cell surface density of CFTR-3HA variants was measured by anti-HA Ab assay using HRP-conjugated goat anti–mouse secondary Ab (GE Healthcare) and Amplex Red (Invitrogen) as a fluorescent substrate. The fluorescence was measured by a plate reader (POLARstar OPTIMA; BMG Labtech, Inc.) using 544-nm excitation and 590-nm emission wavelengths. Specific binding of the anti-HA Ab was calculated by correcting the signal with the nonspecific adsorption of the secondary Ab. Cell surface density of CFTR was normalized by protein concentration based on BCA assay. Internalization of CFTR was calculated from the difference of specific anti-HA Ab binding before and after endocytosis at 37°C for 5 min. All experiments were performed using three or four parallel samples at least three times.

CFTR recycling assay

CFTR recycling efficiency was measured as described previously (Sharma et al., 2004) with modifications. Cell surface CFTR was labeled with anti-HA Ab (0°C for 1 h) followed by labeling of biotin-conjugated anti–mouse Fab (0°C for 1 h; 216–1,806 aa; KPL, Inc.). CFTR was internalized at 37°C for 30 min in the complete culture medium, and the remaining cell surface–associated Ab was blocked by streptavidin (10 µg/ml at 0°C; Sigma-Aldrich). To induce the recycling, the cells were incubated in complete culture medium for 10 min at 37°C. The amount of recycled CFTR–Ab complex was measured by HRP-NeutrAvidin (Thermo Fisher Scientific) using Amplex Red.

siRNA transfection

CNX depletion of HeLa cells stably expressing CFTR-3HA was achieved by the CNX-specific ON-TARGET plus SMARTpool siRNA (100 nM final concentration; Thermo Fisher Scientific) using Oligofectamine (Invitrogen) transfection. Cells were trypsinized 24 h after the first transfection and retransfected after 24 h of seeding. 24 h after the second transfection, cells were split into two 6-cm dishes for pulse-chase experiments. CNX knockdown efficiency was examined by Western blot analysis in parallel samples. TSG101 and Hrs depletion of HEK293 cells transiently expressing wt and 2D-CFTR was achieved by the specific ON-TARGET plus SMARTpool siRNA (50 nM final concentration) using Oligofectamine and verified by using rabbit anti-Hrs Ab (provided by H. Stenmark, University of Oslo, Montebello, Norway) and anti-TSG101 Ab (4A10; GeneTex, Inc.). For Hrs depletion, siRNA was retransfected 2 d after the first siRNA transfection. Control cells were treated with Non-Targeting siRNAs (Thermo Fisher Scientific). All experiments were performed 4 d after the first transfection.

Measurement of ubiquitination of CFTR in post-Golgi compartments

Ubiquitination level of CFTR variants in post-Golgi compartments of BHK cells was measured as described previously (Sharma et al., 2004). 2D-CFTR was rescued by 26°C incubation for 24 h with 10% glycerol followed by 37°C incubation for 3 h without glycerol in the presence of 100–150 µg/ml CHX for 3 h to eliminate the immature CFTR from the ER (Fig. S1 F).

pH_v measurement of CFTR containing endocytic organelles

The pH of endocytic vesicles (pH_v) containing CFTR variants was measured by FRIA as described previously (Sharma et al., 2004; Barriere et al., 2007).

In situ protease susceptibility of CFTR

In situ protease susceptibility of CFTR was determined as described previously (Du et al., 2005). Microsomes were isolated from transfected BHK cells by nitrogen cavitation and differential centrifugation (Zhang et al.,

1998). The core-glycosylated nonnative wt and 2D-CFTR was eliminated from the cells during 2.5–3-h incubation in the presence of 150 µg/ml CHX before microsome isolation. Digested microsomes were immediately dissolved in 2× Laemmli sample buffer (LSB) at 25°C for 10 min and subjected to immunoblot analysis. Proteolytic digestion patterns were visualized by immunoblotting, using the mouse monoclonal M3A7, 660, and MM13-4, and anti-HA Abs, recognizing epitopes in the NBD2, NBD1, MSD1, N-terminal tail, and MSD2, respectively (Cui et al., 2007).

Glycosidase digestion

To remove unprocessed N-glycans and all types of N-glycans, cell lysates were incubated with 7 µg/ml endo H (50 U total activity; New England Biolabs, Inc.) and 31 µg/ml PNGase F (500 U; New England Biolabs, Inc.), respectively, for 3 h at 33°C. Deglycosylation of wt and mutant CFTR at the cell surface was achieved by exposing the cells to recombinant PNGase enzyme (0.5–0.8 mg/ml PNGase [1:50 vol/vol]) in DMEM/F-12 medium supplemented with 10% FBS. To avoid newly synthesized channel delivery, cells were preincubated for 1.5 h with 100 µg/ml CHX. The mobility shift of deglycosylated CFTR was visualized by immunoblotting. The digestion of high mannose–type oligosaccharides containing CFTR at the cell surface was achieved by exposing the transfected HEK293S cells to 2 mg/ml recombinant endo A (endo M, endo-β-N-acetylglucosaminidase) for 2 h after pretreatment for 1.5 h with CHX. Recombinant PNGase and endo A enzymes were purified from *Escherichia coli*. The pMAL-p2/PNGase F expression vector was obtained from P. Van Roey (Wadsworth Center, Albany, NY). The vector produces a maltose-binding protein fusion of PNGase F that is secreted into the periplasm of *E. coli*. The GST–endo A expression vector was obtained from K. Takegawa (Kagawa University, Kagawa, Japan; Fujita et al., 2000). It produces a GST–endo A fusion protein that is expressed in the cytoplasm of *E. coli*. Fusion proteins were purified by affinity chromatography.

Iodide efflux assay

The plasma membrane cAMP-dependent halide conductance of transfected BHK cells was determined with iodide efflux as described previously (Sharma et al., 2001). The parental BHK cells have no cAMP-activated halide conductance.

Immunofluorescence microscopy

Immunostaining of cell surface CFTR variants in BHK cells was performed as described previously (Sharma et al., 2004). Plasma membrane of nonpermeabilized cells was stained with 2 µg/ml Alexa Fluor 594–WGA. Intracellular destination of internalized CFTR was examined by colocalization of labeled CFTR (1-h labeling in the presence of anti-HA and tetramethylrhodamine-labeled secondary IgG or Fab followed by 30-min chase at 37°C) with 25 µg/ml FITC-dextran–loaded lysosomes (37°C overnight labeling and 3-h chase; molecular mass, 10 kD; Invitrogen). Recycling endosomes were identified by 15 µg/ml FITC-transferrin (1 h at 37°C; Sharma et al., 2004). Single optical sections were collected on an inverted laser confocal fluorescence microscope (LSM 510; Carl Zeiss, Inc.) equipped with a Plan-Apochromat 63×/NA 1.4 objective in multitrack mode. Images were processed by Photoshop (version 9; Adobe).

Immunoprecipitation

Cells were solubilized in lysis buffer (25 mM Tris-Cl, 150 mM NaCl, 0.1% NP-40, 10 mM $CaCl_2$, pH 7.4, supplemented with 1 mM PMSF, 5 µg/ml leupeptin, and pepstatin), and precleaned lysates were used for immunoprecipitation with anti-CFTR antibodies (M3A7 and L12B4). Immune complexes were collected on protein G Agarose (Invitrogen) and washed five times with lysis buffer. Complexes were eluted in LSB and analyzed by immunoblotting.

Statistical analysis

Experiments were repeated at least three times, and data were expressed as means ± SEM. Two-tailed p-values were calculated at 95% confidence levels with unpaired *t* test using the Prism software (GraphPad Software, Inc.).

Online supplemental material

Fig. S1 shows that glycosylation mutations attenuate the expression but have no major effect on the translational rate, ERAD kinetics, and the ER exit of the channel. Fig. S2 shows that short treatment of the cells with TUN and CAS does not provoke an ER stress response. CAS, besides decreasing the folding efficiency, also accelerates CFTR posttranslational folding kinetic. Fig. S3 illustrates that removal of N-glycans from native CFTR does not affect the CFTR stability at the cell surface. Fig. S4 demonstrates that preventing N-glycosylation increases the global and local chymotrypsin susceptibility of CFTR. Fig. S5 shows the effect of inserting an additional N-glycosylation site into the fourth loop on the expression and folding efficiency of 900D- and 2D-CFTR. Online supplemental material is available at http://www.jcb.org/cgi/content/full/jcb.200808124/DC1.

We thank H. Stenmark and J. Riordan for antibodies, P. Van Roey and K. Takegawa for plasmids, G. Khorana for HEK293S cells, and K. Du for the construction of the 2A- and 2Q-CFTR. We are grateful to W.E. Balch for valuable suggestions and to I. Braakman, P. Thomas, and W. Skach for stimulating discussions.

T. Okiyoneda was supported by a Canadian CF Foundation postdoctoral fellowship. This work was supported by grants to G.L. Lukacs and J. Rini from the Canadian Institutes of Health Research, the National Institutes of Health (National Institute of Diabetes and Digestive and Kidney Diseases), CF Foundation Therapeutics, the Canadian CF Foundation, and the Canadian Foundation for Innovation. G.L. Lukacs is a holder of a Canada Research Chair.

Submitted: 25 August 2008
Accepted: 24 February 2009

References

Agashe, V.R., S. Guha, H.C. Chang, P. Genevaux, M. Hayer-Hartl, M. Stemp, C. Georgopoulos, F.U. Hartl, and J.M. Barral. 2004. Function of trigger factor and DnaK in multidomain protein folding: increase in yield at the expense of folding speed. *Cell.* 117:199–209.

Arvan, P., X. Zhao, J. Ramos-Castaneda, and A. Chang. 2002. Secretory pathway quality control operating in Golgi, plasmalemmal, and endosomal systems. *Traffic.* 3:771–780.

Asano, T., K. Takata, H. Katagiri, H. Ishihara, K. Inukai, M. Anai, H. Hirano, Y. Yazaki, and Y. Oka. 1993. The role of N-glycosylation in the targeting and stability of GLUT1 glucose transporter. *FEBS Lett.* 324:258–261.

Balch, W.E., R.I. Morimoto, A. Dillin, and J.W. Kelly. 2008. Adapting proteostasis for disease intervention. *Science.* 319:916–919.

Barriere, H., C. Nemes, K. Du, and G.L. Lukacs. 2007. Plasticity of polyubiquitin recognition as lysosomal targeting signals by the endosomal sorting machinery. *Mol. Biol. Cell.* 18:3952–3965.

Bechtluft, P., R.G. van Leeuwen, M. Tyreman, D. Tomkiewicz, N. Nouwen, H.L. Tepper, A.J. Driessen, and S.J. Tans. 2007. Direct observation of chaperone-induced changes in a protein folding pathway. *Science.* 318:1458–1461.

Benharouga, M., M. Sharma, J. So, M. Haardt, L. Drzymala, M. Popov, B. Schwapach, S. Grinstein, K. Du, and G.L. Lukacs. 2003. The role of the C terminus and Na+/H+ exchanger regulatory factor in the functional expression of cystic fibrosis transmembrane conductance regulator in nonpolarized cells and epithelia. *J. Biol. Chem.* 278:22079–22089.

Chang, X.B., A. Mengos, Y.X. Hou, L. Cui, T.J. Jensen, A. Aleksandrov, J.R. Riordan, and M. Gentzsch. 2008. Role of N-linked oligosaccharides in the biosynthetic processing of the cystic fibrosis membrane conductance regulator. *J. Cell Sci.* 121:2814–2823.

Chen, G., O. Frohlich, Y. Yang, J.D. Klein, and J.M. Sands. 2006. Loss of N-linked glycosylation reduces urea transporter UT-A1 response to vasopressin. *J. Biol. Chem.* 281:27436–27442.

Cheng, S.H., R.J. Gregory, J. Marshall, S. Paul, D.W. Souza, G.A. White, C.R. O'Riordan, and A.E. Smith. 1990. Defective intracellular transport and processing of CFTR is the molecular basis of most cystic fibrosis. *Cell.* 63:827–834.

Christianson, J.C., T.A. Shaler, R.E. Tyler, and R.R. Kopito. 2008. OS-9 and GRP94 deliver mutant alpha1-antitrypsin to the Hrd1-SEL1L ubiquitin ligase complex for ERAD. *Nat. Cell Biol.* 10:272–282.

Conti, L.R., C.M. Radeke, and C.A. Vandenberg. 2002. Membrane targeting of ATP-sensitive potassium channel. Effects of glycosylation on surface expression. *J. Biol. Chem.* 277:25416–25422.

Cronin, N.B., A. O'Reilly, H. Duclohier, and B.A. Wallace. 2005. Effects of deglycosylation of sodium channels on their structure and function. *Biochemistry.* 44:441–449.

Cui, L., L. Aleksandrov, X.B. Chang, Y.X. Hou, L. He, T. Hegedus, M. Gentzsch, A. Aleksandrov, W.E. Balch, and J.R. Riordan. 2007. Domain interdependence in the biosynthetic assembly of CFTR. *J. Mol. Biol.* 365:981–994.

daCosta, C.J., D.E. Kaiser, and J.E. Baenziger. 2005. Role of glycosylation and membrane environment in nicotinic acetylcholine receptor stability. *Biophys. J.* 88:1755–1764.

Du, K., M. Sharma, and G.L. Lukacs. 2005. The DeltaF508 cystic fibrosis mutation impairs domain-domain interactions and arrests post-translational folding of CFTR. *Nat. Struct. Mol. Biol.* 12:17–25.

Ellgaard, L., and A. Helenius. 2003. Quality control in the endoplasmic reticulum. *Nat. Rev. Mol. Cell Biol.* 4:181–191.

Fan, J.Q., K. Takegawa, S. Iwahara, A. Kondo, I. Kato, C. Abeygunawardana, and Y.C. Lee. 1995. Enhanced transglycosylation activity of Arthrobacter protophormiae endo-beta-N-acetylglucosaminidase in media containing organic solvents. *J. Biol. Chem.* 270:17723–17729.

Farinha, C.M., and M.D. Amaral. 2005. Most F508del-CFTR is targeted to degradation at an early folding checkpoint and independently of calnexin. *Mol. Cell. Biol.* 25:5242–5252.

Free, R.B., L.A. Hazelwood, D.M. Cabrera, H.N. Spalding, Y. Namkung, M.L. Rankin, and D.R. Sibley. 2007. D1 and D2 dopamine receptor expression is regulated by direct interaction with the chaperone protein calnexin. *J. Biol. Chem.* 282:21285–21300.

Fujita, K., N. Tanaka, M. Sano, I. Kato, Y. Asada, and K. Takegawa. 2000. Synthesis of neoglycoenzymes with homogeneous N-linked oligosaccharides using immobilized endo-beta-N-acetylglucosaminidase A. *Biochem. Biophys. Res. Commun.* 267:134–138.

Gong, Q., C.L. Anderson, C.T. January, and Z. Zhou. 2002. Role of glycosylation in cell surface expression and stability of HERG potassium channels. *Am. J. Physiol. Heart Circ. Physiol.* 283:H77–H84.

Hammerle, M.M., A.A. Aleksandrov, X.B. Chang, and J.R. Riordan. 2000. A novel CFTR disease-associated mutation causes addition of an extra N-linked oligosaccharide. *Glycoconj. J.* 17:807–813.

Harada, K., T. Okiyoneda, Y. Hashimoto, K. Ueno, K. Nakamura, K. Yamahira, T. Sugahara, T. Shuto, I. Wada, M.A. Suico, and H. Kai. 2006. Calreticulin negatively regulates the cell surface expression of cystic fibrosis transmembrane conductance regulator. *J. Biol. Chem.* 281:12841–12848.

Helenius, A., and M. Aebi. 2001. Intracellular functions of N-linked glycans. *Science.* 291:2364–2369.

Helenius, A., and M. Aebi. 2004. Roles of N-linked glycans in the endoplasmic reticulum. *Annu. Rev. Biochem.* 73:1019–1049.

Hendriks, G., M. Koudijs, B.W. van Balkom, V. Oorschot, J. Klumperman, P.M. Deen, and P. van der Sluijs. 2004. Glycosylation is important for cell surface expression of the water channel aquaporin-2 but is not essential for tetramerization in the endoplasmic reticulum. *J. Biol. Chem.* 279:2975–2983.

Imperiali, B., and S.E. O'Connor. 1999. Effect of N-linked glycosylation on glycopeptide and glycoprotein structure. *Curr. Opin. Chem. Biol.* 3:643–649.

Kornfeld, R., and S. Kornfeld. 1985. Assembly of asparagine-linked oligosaccharides. *Annu. Rev. Biochem.* 54:631–664.

Krebs, M.P., S.M. Noorwez, R. Malhotra, and S. Kaushal. 2004. Quality control of integral membrane proteins. *Trends Biochem. Sci.* 29:648–655.

Kumar, K.G., H. Barriere, C.J. Carbone, J. Liu, G. Swaminathan, P. Xu, Y. Li, D.P. Baker, J. Peng, G.L. Lukacs, and S.Y. Fuchs. 2007. Site-specific ubiquitination exposes a linear motif to promote interferon-α receptor endocytosis. *J. Cell Biol.* 179:935–950.

Lau, K.S., E.A. Partridge, A. Grigorian, C.I. Silvescu, V.N. Reinhold, M. Demetriou, and J.W. Dennis. 2007. Complex N-glycan number and degree of branching cooperate to regulate cell proliferation and differentiation. *Cell.* 129:123–134.

Loo, M.A., T.J. Jensen, L. Cui, Y. Hou, X.B. Chang, and J.R. Riordan. 1998. Perturbation of Hsp90 interaction with nascent CFTR prevents its maturation and accelerates its degradation by the proteasome. *EMBO J.* 17:6879–6887.

Lukacs, G.L., A. Mohamed, N. Kartner, X.B. Chang, J.R. Riordan, and S. Grinstein. 1994. Conformational maturation of CFTR but not its mutant counterpart (delta F508) occurs in the endoplasmic reticulum and requires ATP. *EMBO J.* 13:6076–6086.

Meacham, G.C., Z. Lu, S. King, E. Sorscher, A. Tousson, and D.M. Cyr. 1999. The Hdj-2/Hsc70 chaperone pair facilitates early steps in CFTR biogenesis. *EMBO J.* 18:1492–1505.

Meacham, G.C., C. Patterson, W. Zhang, J.M. Younger, and D.M. Cyr. 2001. The Hsc70 co-chaperone CHIP targets immature CFTR for proteasomal degradation. *Nat. Cell Biol.* 3:100–105.

Melikian, H.E., S. Ramamoorthy, C.G. Tate, and R.D. Blakely. 1996. Inability to N-glycosylate the human norepinephrine transporter reduces protein stability, surface trafficking, and transport activity but not ligand recognition. *Mol. Pharmacol.* 50:266–276.

Mitra, N., S. Sinha, T.N. Ramya, and A. Surolia. 2006. N-linked oligosaccharides as outfitters for glycoprotein folding, form and function. *Trends Biochem. Sci.* 31:156–163.

Mochizuki, K., T. Kagawa, A. Numari, M.J. Harris, J. Itoh, N. Watanabe, T. Mine, and I.M. Arias. 2007. Two N-linked glycans are required to maintain the transport activity of the bile salt export pump (ABCB11) in MDCK II cells. *Am. J. Physiol. Gastrointest. Liver Physiol.* 292:G818–G828.

Molinari, M. 2007. N-glycan structure dictates extension of protein folding or onset of disposal. *Nat. Chem. Biol.* 3:313–320.

Morito, D., K. Hirao, Y. Oda, N. Hosokawa, F. Tokunaga, D.M. Cyr, K. Tanaka, K. Iwai, and A.K. Nagata. 2008. Gp78 cooperates with RMA1 in endoplasmic reticulum-associated degradation of CFTRDeltaF508. *Mol. Biol. Cell.* 19:1328–1336.

Nakatsukasa, K., and J.L. Brodsky. 2008. The recognition and retrotranslocation of misfolded proteins from the endoplasmic reticulum. *Traffic.* 9:861–870.

O'Connor, S.E., and B. Imperiali. 1996. Modulation of protein structure and function by asparagine-linked glycosylation. *Chem. Biol.* 3:803–812.

Oda, Y., N. Hosokawa, I. Wada, and K. Nagata. 2003. EDEM as an acceptor of terminally misfolded glycoproteins released from calnexin. *Science.* 299:1394–1397.

Okiyoneda, T., K. Harada, M. Takeya, K. Yamahira, I. Wada, T. Shuto, M.A. Suico, Y. Hashimoto, and H. Kai. 2004. Delta F508 CFTR pool in the endoplasmic reticulum is increased by calnexin overexpression. *Mol. Biol. Cell.* 15:563–574.

Okiyoneda, T., A. Niibori, K. Harada, T. Kohno, M. Michalak, M. Duszyk, I. Wada, M. Ikawa, T. Shuto, M.A. Suico, and H. Kai. 2008. Role of calnexin in the ER quality control and productive folding of CFTR; differential effect of calnexin knockout on wild-type and DeltaF508 CFTR. *Biochim. Biophys. Acta.* 1783:1585–1594.

Pind, S., J.R. Riordan, and D.B. Williams. 1994. Participation of the endoplasmic reticulum chaperone calnexin (p88, IP90) in the biogenesis of the cystic fibrosis transmembrane conductance regulator. *J. Biol. Chem.* 269:12784–12788.

Raiborg, C., T.E. Rusten, and H. Stenmark. 2003. Protein sorting into multivesicular endosomes. *Curr. Opin. Cell Biol.* 15:446–455.

Rands, E., M.R. Candelore, A.H. Cheung, W.S. Hill, C.D. Strader, and R.A. Dixon. 1990. Mutational analysis of beta-adrenergic receptor glycosylation. *J. Biol. Chem.* 265:10759–10764.

Reeves, P.J., N. Callewaert, R. Contreras, and H.G. Khorana. 2002. Structure and function in rhodopsin: high-level expression of rhodopsin with restricted and homogeneous N-glycosylation by a tetracycline-inducible N-acetylglucosaminyltransferase I-negative HEK293S stable mammalian cell line. *Proc. Natl. Acad. Sci. USA.* 99:13419–13424.

Rosser, M.F., D.E. Grove, L. Chen, and D.M. Cyr. 2008. Assembly and misassembly of cystic fibrosis transmembrane conductance regulator: folding defects caused by deletion of F508 occur before and after the calnexin-dependent association of membrane spanning domain (MSD) 1 and MSD2. *Mol. Biol. Cell.* 19:4570–4579.

Saksena, S., J. Sun, T. Chu, and S.D. Emr. 2007. ESCRTing proteins in the endocytic pathway. *Trends Biochem. Sci.* 32:561–573.

Serohijos, A.W., T. Hegedus, A.A. Aleksandrov, L. He, L. Cui, N.V. Dokholyan, and J.R. Riordan. 2008. Phenylalanine-508 mediates a cytoplasmic-membrane domain contact in the CFTR 3D structure crucial to assembly and channel function. *Proc. Natl. Acad. Sci. USA.* 105:3256–3261.

Sharma, M., M. Benharouga, W. Hu, and G.L. Lukacs. 2001. Conformational and temperature-sensitive stability defects of the delta F508 cystic fibrosis transmembrane conductance regulator in post-endoplasmic reticulum compartments. *J. Biol. Chem.* 276:8942–8950.

Sharma, M., F. Pampinella, C. Nemes, M. Benharouga, J. So, K. Du, K.G. Bache, B. Papsin, N. Zerangue, H. Stenmark, and G.L. Lukacs. 2004. Misfolding diverts CFTR from recycling to degradation: quality control at early endosomes. *J. Cell Biol.* 164:923–933.

Shental-Bechor, D., and Y. Levy. 2008. Effect of glycosylation on protein folding: a close look at thermodynamic stabilization. *Proc. Natl. Acad. Sci. USA.* 105:8256–8261.

Slagsvold, T., K. Pattni, L. Malerod, and H. Stenmark. 2006. Endosomal and non-endosomal functions of ESCRT proteins. *Trends Cell Biol.* 16:317–326.

Traub, L.M., and G.L. Lukacs. 2007. Decoding ubiquitin sorting signals for clathrin-dependent endocytosis by CLASPs. *J. Cell Sci.* 120:543–553.

Vagin, O., S. Turdikulova, and G. Sachs. 2004. The H,K-ATPase beta subunit as a model to study the role of N-glycosylation in membrane trafficking and apical sorting. *J. Biol. Chem.* 279:39026–39034.

Wang, X., J. Matteson, Y. An, B. Moyer, J.S. Yoo, S. Bannykh, I.A. Wilson, J.R. Riordan, and W.E. Balch. 2004. COPII-dependent export of cystic fibrosis transmembrane conductance regulator from the ER uses a di-acidic exit code. *J. Cell Biol.* 167:65–74.

Ward, C.L., and R.R. Kopito. 1994. Intracellular turnover of cystic fibrosis transmembrane conductance regulator. Inefficient processing and rapid degradation of wild-type and mutant proteins. *J. Biol. Chem.* 269:25710–25718.

Watanabe, I., J. Zhu, E. Recio-Pinto, and W.B. Thornhill. 2004. Glycosylation affects the protein stability and cell surface expression of Kv1.4 but not Kv1.1 potassium channels. A pore region determinant dictates the effect of glycosylation on trafficking. *J. Biol. Chem.* 279:8879–8885.

Wiseman, R.L., E.T. Powers, J.N. Buxbaum, J.W. Kelly, and W.E. Balch. 2007. An adaptable standard for protein export from the endoplasmic reticulum. *Cell.* 131:809–821.

Wormald, M.R., and R.A. Dwek. 1999. Glycoproteins: glycan presentation and protein-fold stability. *Structure.* 7:R155–R160.

Yang, Y., S. Janich, J.A. Cohn, and J.M. Wilson. 1993. The common variant of cystic fibrosis transmembrane conductance regulator is recognized by hsp70 and degraded in a pre-Golgi nonlysosomal compartment. *Proc. Natl. Acad. Sci. USA.* 90:9480–9484.

Younger, J.M., L. Chen, H.Y. Ren, M.F. Rosser, E.L. Turnbull, C.Y. Fan, C. Patterson, and D.M. Cyr. 2006. Sequential quality-control checkpoints triage misfolded cystic fibrosis transmembrane conductance regulator. *Cell.* 126:571–582.

Zhang, F., N. Kartner, and G.L. Lukacs. 1998. Limited proteolysis as a probe for arrested conformational maturation of delta F508 CFTR. *Nat. Struct. Biol.* 5:180–183.

Zhu, L., G.F. Jang, B. Jastrzebska, S. Filipek, S.E. Pearce-Kelling, G.D. Aguirre, R.E. Stenkamp, G.M. Acland, and K. Palczewski. 2004. A naturally occurring mutation of the opsin gene (T4R) in dogs affects glycosylation and stability of the G protein-coupled receptor. *J. Biol. Chem.* 279:53828–53839.

Zielenski, J., and L.C. Tsui. 1995. Cystic fibrosis: genotypic and phenotypic variations. *Annu. Rev. Genet.* 29:777–807.